Department of Electronic &Computer Engineering

NNAMDI AZIKIWE UNIVERSITY

PMB 5025, AWKA, ANAMBRA STATE, NIGERIA

FINAL REPORT

FOR

TITLE OF RESEARCH

The Development of a User-Centric Based Clustering Scheme and Spatial Resource Allocation Technique for Mitigation of Interference in 5G Networks

AREA OF RESEARCH: 5G Deployment in Nigeria

Lead Researcher: Engr. Dr. Obinna S. Oguejiofor

Mobile: +2347065931945

Email: os.oguejiofor@unizik.edu.ng

EXECUTIVE SUMMARY

5G cellular network promises to perform better than its predecessor (1G, 2G, 3G, and 4G) in terms of delivering high data rate, improved quality of experience (QoE), high spectral efficiency (SE), improved energy efficiency (EE), etc. However, as the reuse-one deployment of 5G is gradually taking shape all over the world, achieving spectral efficiency and tackling inter-cell interference have become some of the greatest challenges encountered because they reduce user equipment (UE) performance and the overall system performance. Interference can be simply defined in wireless communication as an unwanted signal that corrupts the desired signal, thereby reducing the quality of the desired signal.

Many interference-mitigating schemes have been developed to solve the issue of inter-cell interference, however, while these interference-mitigating techniques improve the performance of the system, some do sacrifice the aggregate spectral efficiency of the system.

In this report, we show how schemes were developed to mitigate both inter-cell interference and as well, improve the system-wide spectral efficiency.

To achieve that, we devised a user-centric-based dynamic clustering scheme, which can determine the optimum number of base stations (BSs) that are interfering with a particular user at a particular time. After this is determined, the interfered user sends a report containing channel state information (CSI) belonging to all interfering BSs to its serving base station, requesting it to cooperate with these interfering BSs to coordinate their resource allocations (RA) in terms of spatial directions to mitigate the inter-cell interference. To validate the resource allocation algorithm devised in this work, a transmitter incorporating a multi-antenna system was designed and developed using software-defined radio and other techniques to validate the algorithm.

The outcome of this project will help in achieving improved quality of experience most especially for UEs at cell edges or cell range expansion areas and also improve the overall system-wide spectral efficiency. This work will be beneficial to the network service providers as well as the mobile network subscribers.

Contents

Executive Summary 1

Background of the Research 4

Statement of the Problem 5

SECTION ONE: STAGE ONE DELIVERABLE REPORTS

1.1 Review of Related Literature 6

1.2 Theoretical Framework 9

1.3 5G System Model Representation and Description 15

1.4 Mathematical Models Based on 5G Heterogeneous System 16

SECTION TWO: STAGE TWO DELIVERABLE REPORTS

2.1 User-Centric Based Clustering Scheme Development 21

SECTION THREE: STAGE THREE DELIVERABLE REPORTS

3.1 Resource Allocation 23

3.2 Problem Formulation 23

3.3 Spatial Direction Allocation Problem 25

3.4 Power Allocation Problem 26

3.5 Algorithm 3.1 27

3.6a Results obtained from our published work 28

3.6b Results obtained from our published work 32

SECTION FOUR: STAGE FOUR DELIVERABLE REPORTS

4.1 Introduction 38

4.2 Design and Development of Transmitter Incorporating Multi-Antenna System 40

4.3 Multi-Antenna System External Power Supply Unit 46

4.4 Receiver Unit 59

4.5 Network Visualizer Unit 65

SECTION FIVE: SUMMARY AND CONCLUSION

5.1 Summary of Findings 70

5.2 Conclusion 70

Acronyms and Notations 71

References 73

Background of the Research

The fifth-generation mobile communication network (5G) technologies are believed to address issues such as inadequate capacity, low data rate, decreased latency, poor quality of service/experience, etc. As the deployment of 5G is gradually taking shape all over the world, achieving spectral efficiency and dealing with interference have become one of the greatest challenges encountered. The evolution of 5G demands a significant increase in spectral efficiency compared to the 4G. It is known that the spectral efficiency of a cellular network can be improved by increasing the cell density through cell splitting, however, its achievable gain as stated above would be significantly limited by severe inter-cell interference.

5G architecture is densely heterogeneous: meaning that each macro-cell has small cells underlaid within it. If all the cells use the same frequency resource, there will be a lot of co-tier/inter-cell interference. To overcome co-channel or inter-cell interference, classical/ traditional mobile communication networks have employed different kinds of techniques: such as dividing the spectrum into different bands so that each cell uses a different radio frequency different from the neighboring cells. We have noticed that such orthogonal deployments improve performance, however, it leads to a low spectral efficiency of the system. Inter-cell interference coordination (ICIC) schemes defined in Release 8 were proposed and introduced in the 4G LTE systems to deal with inter-cell interference problems. Also, Enhanced ICIC (eICIC) schemes defined in Release 10 were proposed and introduced in the 4G LTE Advanced system to deal with inter-cell interference problems as well. These schemes help to coordinate interference but sacrifice the spectrum. Spectral efficiency is one of the major metrics used to evaluate the performance of present and future-generation mobile communication networks. Hence, it is important to develop schemes that can curb both inter-cell interference and improve the system-wide spectral efficiency.

We provide such a solution to the above interference problem by developing a user-centric dynamic clustering scheme, which can determine the optimum number of base stations (BSs) that are interfering with a particular user at a particular time. After this is determined, the interfered user sends a report containing channel state information (CSI) belonging to all interfering BSs to its serving base station, requesting it to cooperate with these interfering BSs to coordinate their resource allocations (RA) in terms of spatial directions to mitigate inter-cell interference. This approach is based on a multi-cell processing policy, which combines multiple-input multiple-output (MIMO) and cooperating techniques to solve the interference issue, improve the quality of experience of the user as well and maximize the system-wide spectral efficiency of the 5G network.

Statement of the Problem

In a classical/conventional system, interference management is achieved by a dense frequency reuse pattern with the base station having a single-cell processing policy (SCP), meaning that user equipment (UEs) in a cell are served by base stations located at the center of the cell only. Furthermore, base stations are not supposed to take care of the links to and from the neighboring cells which contain inter-cell interference. Inter-cell interference is normally

handled by careful frequency planning and allocation. This frequency allocation scheme to each cell and UEs is usually computed and evaluated during the radio planning process and only long-term readjustment is performed during the operation of the network. However, because the need for high-rate wireless communication is ever-growing and due to the scarcity of spectrum in the sub-6 GHz band, Universal frequency reuse has been proposed for LTE-Advanced networks, 5G networks, and future networks. In this context, UEs, whose base stations use a single-cell processing policy will experience strong inter-cell interference from neighboring cells. Particularly, cell-edge UEs or UEs at the cell range expansion area of small cells will receive signals with low signal-to-interference-and-noise-ratio (SINR) and poor quality as a result of signal attenuation from their serving base stations and inter-cell interference from neighboring cells.

SECTION ONE: STAGE ONE DELIVERABLE REPORTS

1.1 Review of related literature

5G heterogeneous network consists of both the macro base station and the small cell base stations operating together in a single band. This research is aware of a multi-band heterogeneous network with inter-site carrier aggregation, where macro base station and small cell base stations use different bands, in this setting, interference mitigation schemes are not needed, however, it will lead to the development of a new type of user equipment (UE) which can have dual access to two different bands. We are rather interested in a 5G heterogeneous network operating in a single-band arrangement. Single band network suggests that the same band (C-band) is used by both the macro base station and the small cells base stations. This idea is not recent since it has been standardized in 3GPP release 10. However, it is important due to scarce spectrum allocation, and because the evolution of new-generation mobile communication such as 5G and beyond 5G (B5G) demands a significant increase in spectral efficiency (SE) compared to the one obtained in the current 4G systems hence the need for the maximization of the single band spectrum. However, this arrangement requires interference management schemes to address the resultant inter-cell/inter-tier interference that will occur. Interference is a limiting factor to the performance of most mobile communication networks including 5G Networks [1]. Interference management is one of the most challenging issues facing mobile network operators and if not gotten right can lead to low signal-to-interference-and-noise-ratio (SINR) for UEs and consequently low data rate for the system [2, 3]. Many works have been proposed on how to manage interference from 2G networks up to 5G networks. Classical interference management schemes utilize a single-cell processing policy with careful frequency planning to avoid interference, however, this method is statically done and involves a lot of frequency planning before execution. Its limitation is that it sacrifices the spectrum to control interference. Multi-cell processing (MCP) has emerged as an efficient way to suppress interference as well as enhance the SE of the system [4, 5].

In the MCP, base stations (BSs) cooperate on different levels to manage interference and at the same time improve the individual BSs that form the cluster. Clustering is very important in MCP because it can help to group specific BSs together to mitigate interference and/or improve the received signal quality for UE at the cell edges. Different clustering schemes have been proposed in the literature and they can be categorized as UE-centric clustering [6–8], network-centric clustering [9, 10], and hybrid clustering [11]. In the UE-centric clustering scheme, the UE selects the coordinating BSs based on its point of view, these BSs either serve or reduce interference from it. In contrast, network-centric clustering is performed by the operators on a static or semi-static basis and has been castigated for not fully utilizing the channel variations of UE present in the network, while hybrid clustering will achieve the trade-off between the performance and complexity of the aforementioned clustering schemes.

Coordinated beamforming (CB) [12] is a type of MCP described in the third-generation partnership project (3GPP) LTE-advanced, which requires partial cooperation between the cooperating BSs. In CB, each BS serves its UE with data while control information is exchanged between BSs with which RA decisions can be made collectively. Compared with joint transmission (JT) [13], CB is a practical and feasible approach for mitigating interference in the downlink of single-tier cellular networks [14–17]. JT has limitations from a practical perspective because it requires full phase coherence among signals received from different BSs, which is usually impossible due to the difference in propagation delay. Tight synchronization [18] is a very important factor JT needs to become practically feasible. Some new ideas have emerged on implementing JT using cloud radio access network (RAN) technology [19] and using tools from stochastic geometry [20, 21]. Though the theories behind it make sense, however, the practical implementation is where the problem lies. Even if an unlimited-capacity fiber optical link is utilized for data sharing, it will only increase operational expenditures (OPEX). If the net gain between the OPEX and increased SE is small, then the motivation behind increased expenditure for implementing JT cannot be justified.

Although the effectiveness of CB has been well studied in single-tier homogeneous cellular networks where the multi-cell characteristics and accompanying inter-cell interference (ICI) are usually limited to at most three cooperating macro base stations (MBSs), its application in a densely deployed heterogeneous 5G network scenario requires a detailed investigation.

Previous works on coordinated beamforming either use the Wyner model [22–24], which is a simplified model where interference only comes from the immediate neighboring cells, or a network-centric model [25–27], which is networked with static clusters, this clustering method limits the cooperating area in several fixed BSs thereby cannot flexibly adapt to the changing topology. Furthermore, in [28, 29], BSs are divided into static disjoint cooperation clusters. Each cluster is operated as a single-cell system. However, networks with this kind of cluster usually provide poor spectral efficiency when the UE distribution is heterogeneous, also these clusters suffer from out-of-cluster interference and thereby affect the performance of the system. In [30, 31], UE-centric-based clustering is utilized for ICI nulling. However, this is done for single-tier small-cell networks. Furthermore, in [32, 33], UE-centric-based clustering and beamforming are utilized for energy efficiency optimization; however, this is targeted for cloud RAN. Resource allocation has attracted a lot of attention in the past; however, it is mainly for single-tier networks such as in [12] and references therein. The contributions made in these papers do not address the significant interference problem posed when multi-tier networks are deployed, hence cannot be used in practical realistic multi-tier networks such as 5G heterogeneous networks, which have more significant ICI situations, different propagation characteristics, different cell selection procedures and different BS power classes. We affirm that the major difficulty in the resource allocation facing 5G is the issue of inter-cell interference, which degrades the performance of the 5G networks when the UEs are served in parallel in the same frequency-time resource, for the 5G systems using space-division multiple access (SDMA) in each cell and cooperation among coordinating BSs. Recently, resource allocation (RA) has been investigated for different networks. In [34, 35], RAs were investigated for the uplink of orthogonal frequency-division multiple access networks and two-cell networks, respectively. In [36, 37], their RA optimization problem was similar to ours, in the sense that it was geared towards achieving spectral efficiency, however, the methodology used to actualize it differs. Furthermore, in [38–43], the RA utility function is geared towards achieving energy efficiency in the heterogeneous network. However, this research differs from the aforementioned reviewed papers in the sense that our RA optimization problem is geared towards achieving SE but also constrains the total power at each transmitter to different given values to enable energy efficiency. Furthermore, their RA is done by fixed BSs without considering clustering, which in practice will reduce the improvements they claimed are achievable by their work because of the regular change of the heterogeneous network topology. In contrast, we determine the optimal number of interfering BSs that cause significant interference to each UE based on its point of view. These interfering BSs together with the serving BS of the interfered UE will coordinate and make RA decisions together to mitigate interference and thereby improve the achievable throughput in the 5G network.

We have published some aspects of the concept shared in this research on how to manage interference for different cellular networks in the past and these can be found here [44-53].

1.2 Theoretical Framework

a) Concepts Explanation

From the statement of the problem of this research, the concepts that need explaining include but are not limited to the following:

1. Interference Management: It is one of the most challenging issues facing mobile network operators and if not gotten right can lead to low SINR for UEs and correspondingly low data rate for the system. By interference management, we mean schemes and approaches this research will develop or adopt to tackle interference in 5G heterogeneous networks operating at the C-band.
2. Dense Frequency Reuse: This is an approach used in most conventional cellular networks to manage interference and avoid inter-cell interference. In this approach, the same radio carrier frequency will not be utilized by adjacent cells to avoid co-channel or inter-cell interference. However, the same radio carrier frequency can be reused after some cells based on calculations. This approach is oftentimes regarded as a dense frequency reuse pattern.

In contrast, this research work is focused on a 5G network and will utilize universal frequency reuse also known as frequency reuse-1 deployment.

3. Universal Frequency Reuse: This was implemented starting with 4G networks and will also be utilized for 5G networks, and future networks. In universal frequency reuse, all cells use the same carrier frequency due to the scarcity of spectrum and the need for high-rate wireless communication. The aim is to maximize spectral efficiency; however, this could lead to high levels of inter-cell interference due to simultaneous transmissions on the same frequency by neighboring base stations. In this research work, the universal frequency reuse or frequency reuse-1 was adopted for our 5G system model while developing schemes that will effectively manage the resulting inter-cell interference.
4. Single-cell Processing (SCP): It is terminology in mobile communication networks used for describing base stations that unilaterally serve their user equipment (UE) without considering another source of interference that might affect its UEs but rather treating them as Gaussian noise. Classical mobile networks utilize SCP when communicating with its serve UEs while interference is managed using fixed frequency reuse patterns or power control.
5. Inter-cell Interference (ICI): ICI is the kind of interference that occurs between cells in a multi-cell scenario. The main reason behind the cause of this interference is when cells operate under universal frequency reuse. This will now make it possible for the desired signal that is meant for an UE in cell A to be also received by another UE in cell B which sees it as an undesired signal (interfering signal). Inter-tier, intra-tier, and cross-tier interferences can also be regarded as synonyms for ICI. However, inter-tier or cross-tier interference represents interference between heterogeneous cells, while intra-tier or co-tier interference represents interference between homogeneous cells. For example, see Fig. 1.1 for illustrations of different cases of interference that can happen in the uplink/downlink of a 5G heterogeneous network.

✓ Interference case (1): shows an uplink intra-tier interference of a small cell UE interfering with a nearby small cell base station.

✓ Interference case (2): Shows downlink intra-tier interference of a small cell base station interfering with a nearby small cell UE.

- ✓ Interference case (3): Shows downlink inter-tier interference between the macro base station and a neighboring small cell UE.
- ✓ Interference case (4): illustrates downlink interference from a small cell BS to a macro cell edge UE.

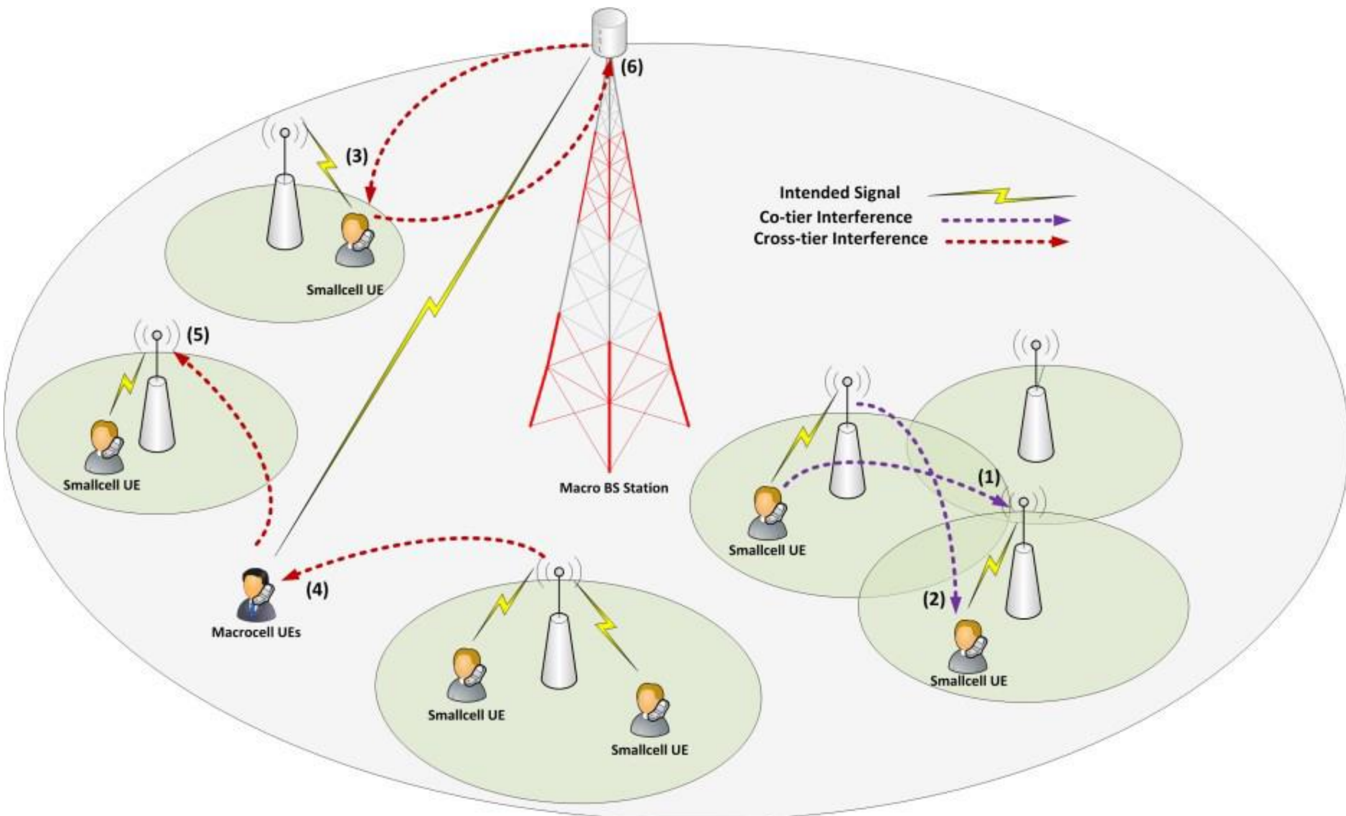

Figure 1.1: Different cases of inter-tier and intra-tier interference in 5G Heterogeneous Network

- ✓ Interference case (5): Illustrates how uplink inter-tier interference occurs when a macro UE is at the cell edge and needs to transmit at high powers to compensate for the high path-loss and shadowing effect.
- ✓ Lastly, interference case (6): Illustrates uplink inter-tier interference between a small cell UE and a neighboring macro base station.

6. Cell Edge UEs: These are UEs that are located towards the edge of the cells, they exhibited much poorer performance than the interior UEs because they suffer from both high signal attenuation and severe inter-cell interference. UEs at the cell edge usually have relatively

similar channel gains from multiple base stations, unlike interior UEs which have only one strong dominating channel from one of the base stations. In this research work, we are more interested in cell edge UEs than interior UEs because they are the one that suffers from ICI.

7. Cell Range Expansion (CRE): It is a terminology often somewhat similar to the cell edge, however, it is usually used for small cells, especially Pico cells. CRE was introduced in the Pico cell to remedy the load balancing problem in the downlink Heterogeneous Network. Its goal is to augment the downlink coverage footprint of small cell base stations (SCBS) by adding positive bias to their reference signal receive power (RSRP). This bias will allow more UEs to be associated with SCBS, thereby achieving improved cell load balancing. The problem with this approach is that it makes serving cell selection more uplink relevant, and the UEs in the CRE have the most favorable downlink from the non-serving MBS, therefore causing huge downlink interference for those UEs. If a UE is located in the region of cell range expansion, it will suffer from severe downlink interference from the macro BS, since it is not connected to the cell that provides the best downlink received signal.
8. System Model: A system in an abstract sense refers to mappings that take a signal as input and produce another signal as an output, it defines the relationship between the inputs and outputs.

   A model is a representation of the given system in the language one can conceive of. A mathematical model is the description of a system using mathematical concepts and languages.

   We describe the system model in this research as a section of a mobile communication network, where research is carried out to provide valuable insight and to enable analysis using mathematical concepts and languages.

9. Clustering is very important in multi-cell processing because it can help group-specific BSs together to mitigate interference and/or improve the received signal quality for UE at the cell edges.

10. Resource Allocation involves strategies and procedures for selecting and apportioning radio resource parameters such as frequency, time, spatial directions, transmit powers, etc. to satisfy the objective of the system designer.

b) Explaining Relevant Theories

This section explains relevant theories and theorems that are related to this research's key concepts. This is important because it will show that this research work is grounded in established ideas.

1. Information Theory: It is a mathematical approach to the study of coding of information in the form of sequences of symbols, impulses, etc. along with quantification, storage, and,

communication of information. The theory is devoted to the discovery and exploration of mathematical laws that govern the behavior of data as it is transferred, stored, or retrieved.

2. Shanon-Hartly Theorem: In Information theory, the Shanon-Hartly Theorem tells the maximum rate at which information can be transmitted over a communication channel of a specified bandwidth in the presence of noise.
3. Computation Complexity Theory: It focuses on classifying computational problems according to their resource usage, and relating these classes to each other. A computational problem is a task solved by a computer. More precisely, computational complexity theory tries to classify problems that can or cannot be solved with appropriately restricted resources.
4. Optimization Theory: It is a branch of mathematics that is focused on solving optimization problems. An optimization problem is a problem where the objective function (utility function) is minimized (maximize) and subject to some constraint functions. Getting the optimization variables is key to finding the optimized value (minimized value or minimum value)
5. Lagrange Multiplier Theorem: It states that at any local maxima (or minima) of the function evaluated under the equality constraints, if constraint qualification applies, then the gradient

of the function (at that point) can be expressed as a linear combination of the gradients of the constraints (at that point) with the Lagrange multipliers acting as a coefficient.

In mathematical optimization, the Lagrange multiplier is a strategy for finding the local maxima and minima of a function subject to equality constraints.

6. Duality Theory: It is a branch of optimization theory that shows that optimization problems may be viewed from either of two perspectives, the primal problem, or the dual problem. If the primal is a minimization problem, then the dual is a maximization problem and vice versa. The solution to the primal problem is an upper bound to the solution of the dual problem, and the solution of the dual problem is a lower bound to the solution of the primal. The optimal values of the optimal and dual problems need not be equal. Their difference is called the duality gap. For convex optimization problems, the duality gap is zero under a constraint qualification condition. This fact is called strong duality.

c) Relationship Between the Aforementioned Existing Theories and this Research

This sub-section discusses how this research utilizes or adapts the aforementioned theories to obtain or analyze results. In some cases, more than one theory was combined uniquely to enhance the interpretation of the results obtained.

1. Information Theory: We applied a part of this theory during the description of our proposed system model. Through mathematical models, we show the input-output relation of the proposed 5G system. The 5G system model is only focused on the radio access network (RAN) which consists of the base stations, the air interface, the user equipment, and their interactions.
2. Shannon-Hartley Theorem: We also applied a part of this theorem when we utilized spectral efficiency as one of the metrics to adjudge the performance of the system considered. Mathematically it can be represented thus: $\log_2\left(1+\frac{Received\ Signal\ Power}{Interference\ Power+Noise\ Power}\right) \quad bits/s/Hz/UE$

3. Computational Complexity Theory: We also utilized a part of this theory when we devised a sub-optimal efficient algorithm using convex optimization, and an optimal inefficient algorithm using global optimization. We utilized the complexity theory to show the
4. complexities of these algorithms and to gain insight into how to utilize them based on the efficiencies of the algorithms.
5. Optimization Theory: We utilized a part of this theory in our devised resource allocation schemes to maximize the spectral efficiency of a 5G heterogeneous system subject to some stated constraints.
6. Lagrange Multiplier Theorem: Most optimization problems can only be solved numerically; however, we utilized this theorem to analytically solve some of the developed optimization problems in this research work.
7. Duality Theory: We applied a part of this theory to solve an NP-hard non-linear optimization problem. Because weak duality allows the use of convex optimization to approximately solve non-convex optimization problems.

1.3 5G System Model Representation and Description

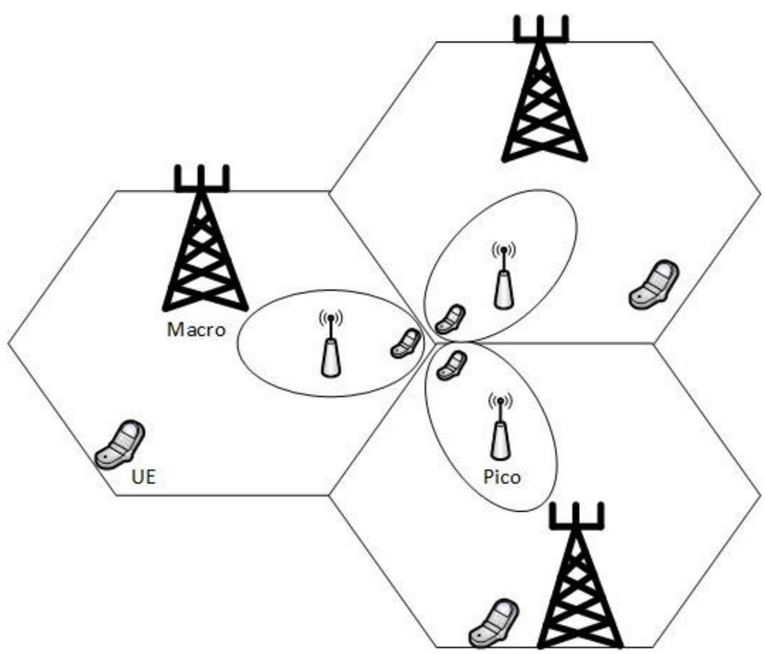

Figure 1.2: Downlink 5G heterogeneous system with Pico cells in the coverage area of MBS

Let's consider the downlink of a 5G heterogeneous network as depicted in Fig. 1.2, which consists of K_p picocells and K_m macro cells making it a total of K_t cells in the system. [Note that the number of pico cells considered for each macro-cell is not limited to one, as suggested by Fig. 1.2 but for clarity, we just showed a simplified schematic representation of our considered system. In our simulation, the total number of pico cells considered will be stated.] We assume that all cells in the 5G heterogeneous network use the same carrier frequency, note that this is not the case in orthogonal frequency-division multiplexing (OFDM) systems. The jth BS is denoted BS_j which can be any of the BSs (PBS or MBS) and is assumed to have N antennas with which it communicates with at least one active UE per cell which is assumed to have a single antenna. [We limit each UE to having a single antenna for practical reasons, such as reducing the UE hardware complexity and preserving battery life]. The set of UEs served by BS_j is denoted by $\mathcal{S}_j \subset \{1, \ldots, K_r\}$, where K_r denotes the total number of UEs in the 5G network, also the kth UE is denoted UE *k*. While the selected n-tuple BSs that interfere with UE *k* is denoted by $\mathcal{C}_n^k$. The main system parameters are listed in Table 1.1. Note that the macro-pico heterogeneous scenario is preferred in this work to the macro-femto heterogeneous scenario because coordination among BSs will be much easier due to the connecting backhaul link, which uses a fiber optical link whereas the macro-femto utilizes an internet connection.

1.4 Mathematical Models Based on the 5G Heterogeneous System Considered

Notations: Upper boldface letters are used for matrices; lowercase boldface letters for (column) vectors and either uppercase or lowercase letters without boldface are used for scalars.

The complex-baseband received signal at UE *k* is $y_k \in \mathbb{C}$ and given by

$$y_k = \sum_{j=1}^{K_t} \sqrt{g_{j,k}} \left(\boldsymbol{h}_{j,k}^s\right)^H \boldsymbol{x}_j + z_k. \tag{1}$$

Where $\sqrt{g_{j,k}}$ is the large-scale path-loss from BS_j to UE *k*. Also $\boldsymbol{h}_{j,k}^{s} \in \mathbb{C}^N$ is the small-scale frequency-flat fading channel vector from BS_j to UE *k*, while $\boldsymbol{x}_j \in \mathbb{C}^N$ is the data

signal vector transmitted at BS_j and intended for it served UEs. Furthermore, $z_k \in \mathbb{C}$ is the additive noise from the surroundings and is modeled as circularly symmetric complex Gaussian, distributed as $z_k \sim \mathbb{C}\mathcal{N}(0, \sigma^2)$, where σ^2 is the noise power. Assuming BS_l is the serving BS of UE *k*, the received signal at UE *k* in Eq. (1) can be rewritten as

$$y_k = \boldsymbol{h}_{l,k}^H \boldsymbol{w}_k s_k + \boldsymbol{h}_{l,k}^H \sum_{\substack{p \in \mathcal{S}_l, \\ p \neq k}} \boldsymbol{w}_p s_p + \sum_{\substack{j \in \mathcal{C}_n^k, \\ j \neq l}} \boldsymbol{h}_{j,k}^H \sum_{\substack{m \in \mathcal{S}_j, \\ m \neq k}} \boldsymbol{w}_m s_m + z_k. \quad (2)$$

Also, the transmitted data signal vector is a linear function of the symbols, i.e., $\boldsymbol{x}_j = \sum_{p \in \mathcal{S}_j} \boldsymbol{w}_p s_p$, where $\boldsymbol{w}_p$ denotes the transmit beamformers for each symbol s_p. The first summand of Eq. (2) is the desired signal transmitted to UE *k* while the second and third summands represent the intra-cell interference caused by co-channel UE within the same BS and the inter-cell interference caused by co-channel UE in different BSs respectively. For a 5G heterogeneous network that uses frequency reuse one deployment, the important issues that need to be addressed are:

- **Issue 1**: how to identify the dominant inter-cell interference from BSs in the 5G heterogeneous network to UE *k*. In other words, which BSs should be selected among the possible *n*-tuple BSs that interfere with UE *k* the most. Any BS whose interference power towards UE *k* is less than or equal to the noise power is regarded as negligible interference and, hence is not to be considered for coordination.

- **Issue 2**: How to jointly design the transmit beamformers (coordinated beamformers), that will spatially separate the transmitted signal vector from the interfering BSs to avoid interference towards UE *k*. Note that these interfering BSs are not fixed but selected for UE *k* by solving **issue 1**.

Table 1.1: Key Parameters and Notations	
K_p	The total number of PBS in the 5G system.
K_m	The total number of MBS in the 5G system.
K_t	The total number of BSs in the 5G system, ($n \leq K_t$)
BS_j	The *j*th BS.
$\mathcal{S}_j$	The set of UEs served by BS_j
N	The total number of transmit antennas at PBS or MBS
K	The total number of active served UEs in each cell.
$\sqrt{g_{j,k}}$	The large-scale path-loss from BS_j to UE *k*.
$\boldsymbol{h}^{s}_{j,k}$	The small-scale (fading) channel vector from BS_j to UE *k*.
$\boldsymbol{x}_j$	The data signal vector transmitted at BS_j and intended for its served UEs.
$\mathcal{C}^{k}_{n}$	The selected *n*-tuple BSs that interfere with UE *k*.
$\mathcal{U}_n$	The collection of all possible *n*-tuple BS subsets.
$\mathcal{C}_n$	Particular *n*-tuple BS subsets.
$\boldsymbol{R}_{j,k} \succeq \boldsymbol{0}$	Means $\boldsymbol{R}_{j,k}$ is a positive semi-definite matrix.
K_r	The total number of UEs in the 5G system
σ^2	The noise Power.
τ_p	The limit of interference power at UE *p*.
q_j	The power limit at BS_j
$(\cdot)^H$	The transpose-conjugate operation
$\lVert\cdot\rVert_2$	The Euclidean norm of a vector

$\lvert\cdot\rvert$	The magnitude of a complex variable
$\mathbb{E}\{\cdot\}$	The statistical expectation over a random variable
$\mathbb{R}_{+}^{N}$	The set of real N-vectors with non-negative elements.
$\mathbb{C}$	The set of complex numbers.
$\mathbb{C}^{N}$	The set of complex N-vectors

Remark 1 (Uplink 5G heterogeneous system)

Let's consider the uplink scenario of a 5G system using Fig. 1.2. Note that since all the base stations in the 5G system share the same bandwidth. BS_l can receive signals from UEs it served (desired signal) and UEs it didn't serve (interfering signal). Mathematically the received signal $\boldsymbol{B}_l \in \mathbb{C}^{N\times 1}$ of this uplink transmission can be represented as:

$$\boldsymbol{B}_l = \boldsymbol{h}_{k,l} s_k + \sum_{\substack{p\in\mathcal{S}_l \\ p\neq k}} \boldsymbol{h}_{p,l} s_p + \sum_{\substack{m\in\mathcal{S}_j \\ j\neq l}} \boldsymbol{h}_{m,l} \sum_{m\neq k} s_m + \boldsymbol{z}_l . \quad \text{(a)}$$

The first summand in Eq. (a) represents the desired signal meant for BS_l and transmitted by UE *k*. The second and third summands represent the intra-cell and inter-cell interfering signals respectively.

For the base station to differentiate between the desired signals and the interfering signals coming from UEs in the 5G system, it has to apply some kind of receive processing technique using a receive beamforming vector ($\boldsymbol{u}$). To get the desired data symbol s_k, each term of Eq. (a) will be multiplied by the received beamforming vector $\boldsymbol{u}^H \in \mathbb{C}^{1\times N}$. Mathematically, it can be represented as: $\widehat{s_k} = \boldsymbol{u}^H \boldsymbol{B}_l$.

Note: The receive beamforming vector can be designed based on the goal as follows:

a. Maximum ratio combining: This technique maximizes the ratio between the received signal power and noise power.

b. Zero-forcing filtering: This technique maximizes the ratio between the received signal power and the interference power.

c. Wiener filtering: This technique balances between maximizing the signal power and suppressing the interference.

Note: This research is more interested in downlink transmission.

SECTION TWO: STAGE TWO DELIVERABLE REPORTS

2.1 User-Centric Based Clustering Scheme

In this section, actions are taken to resolve issue 1. A solution is provided to it by finding an optimal BS subset that will give the aggregate largest interference to UE *k* at a given time slot. An abridged expression of Eq. (2) is now written to show only the summation of inter-cell interference signals,

$$int_{sig} = \sum_{\substack{j \in \mathcal{C}_n^k, \\ j \neq l}} \boldsymbol{h}_{j,k}^H \boldsymbol{x}_j . \tag{3}$$

The inter-cell interference power corresponding to Eq. (3) can be represented by

$$int = \sum_{\substack{j \in \mathcal{C}_n^k, \\ j \neq l}} \left| \boldsymbol{h}_{j,k}^H \boldsymbol{x}_j \right|^2 . \tag{4}$$

Let $\{int_n^k\}_{k \in \mathcal{S}_l}$ denote the set of all aggregate inter-cell interference power calculated from *n*-tuple BSs interfering UE *k* with $n \leq K_t$. It is important to note that for a system that comprises of K_t BSs as shown in Fig. 1.2, there are altogether 2^{K_t} possible subsets. Let $\mho_n$ represent the collection of all possible *n*-tuple BS subsets in the 5G heterogeneous network. The optimal BS subset that will maximize the interference suffered by UE *k* can be expressed as

$$\mathcal{C}_n^{k*} = \underset{\mathcal{C}_n \in \mho_n}{\operatorname{argmax}} \; int_n^k \quad \forall k. \tag{5}$$

To be able to find the optimal number of BSs, in the optimal BS subsets, that will cause the highest interference to UE *k*, one can determine that through the following expression:

$$l_n = \max_{\mathcal{C}_n \in \mho_n} \; int_n^k \tag{6}$$

Where l_n denote the maximum value of the interference generated to UE k by n-tuple BSs. Accordingly, the serving BS to UE k, can choose the optimal number of interfering BSs that it will coordinate with, based on l_n. This can be expressed as

$$n_{opt} = \underset{n=1,\dots,K_{t,}}{\operatorname{argmax}} \; l_n. \tag{7}$$

However, it involves finding $\mathcal{C}_n^{k^*}$ using Eq. (5) and l_n using Eq. (6) for each n, before selecting the optimal one using Eq. (7).

The optimal interfering BS set for UE k is easily found as $\mathcal{C}_{n_{opt}}^{k^*}$,, and the optimal number of interfering BSs that are needed to coordinate interference with the serving BS of UE k is n_{opt}. Consequently, the signal received by UE k after identifying its dominant inter-cell interferers is given by

$$y_k = \boldsymbol{h}_{l,k}^H \boldsymbol{x}_l + \sum_{\substack{j=1, \\ j \in \mathcal{C}_{n_{opt}}^{k^*}}}^{n_{opt}} \boldsymbol{h}_{j,k}^H \boldsymbol{x}_j + z_k. \tag{8}$$

Furthermore, the achievable data rate for UE k in beamforming terms, with s_k normalized to unit power, can also be expressed as

$$r_k = \log_2 \left(1 + \frac{\left| \boldsymbol{h}_{l,k}^H \boldsymbol{w}_k \right|^2}{\sigma^2 + \sum_{p \in \mathcal{S}_l} \left| \boldsymbol{h}_{l,k}^H \boldsymbol{w}_p \right|^2 + \sum_{j=1}^{n_{opt}} \sum_{m \in \mathcal{S}_j} \left| \boldsymbol{h}_{j,k}^H \boldsymbol{w}_m \right|^2} \right). \tag{9}$$

For a particular selected BS subset, the received signal y_k in Eq. (8) suffers from the highest significant inter-cell interference that exists in the system and is peculiar to UE k. The corresponding achievable data rate r_k will diminish if these interference sources are not mitigated. Note that if a significant interference source to UE k is not identified and dealt with, it will hinder the performance of UE k.

The next delivery report presents how issue 2 will be resolved through resource allocation, to make sure that these interference sources are dealt with effectively.

SECTION THREE: STAGE THREE DELIVERABLE REPORTS

3.1 Resource Allocation

In this section, the serving BS of UE k will make resource allocation (RA) decisions together with the selected BS subset that causes interference to UE k. The implementation of this RA needs to be done centrally. In this section, the focus is to achieve the fundamental trade-off between maximizing the spectral efficiency of the 5G heterogeneous network and achieving a minimum performance level for all UEs in the 5G system. This decision is motivated by the poor individual performance of UEs located at the cell edges or cell range expansion (CRE) [51] area of picocells in a macro-pico heterogeneous scenario.

3.2 Problem Formulation

The target is to select $\{\boldsymbol{w}_k\}_{k=1}^{K_r}$ to maximize the weighted sum-rate, while fulfilling some power, QoS, and interference constraints (IC) [52], [53]. It is important to note that the individual rate r_k is a function of the signal-to-interference-and-noise ratio $(SINR_k)$. The optimal interfering BS set $\mathcal{C}_{n_{opt}}^{k^*}$ that affects r_k has been used to determine $SINR_k$ as expressed in Eq. (9) [see stage two deliverable report]. The optimization problem is, therefore, formulated as

$$\underset{\{\boldsymbol{w}_k\}_{k=1}^{K_r}}{\text{maximize}} \quad \sum_{k=1}^{K_r} u_k r_k(\{\boldsymbol{w}_k\}),$$

$$\text{subject to} \quad \mathcal{C}_1 : SINR_k \geq \gamma_k \quad k = 1, \dots, K_r,$$

$$\mathcal{C}_2 : \textstyle\sum_{k \in \mathcal{S}_s} \|\boldsymbol{w}_k\|_2^2 \leq q_s \quad s = 1, \dots, K_p, \qquad (10)$$

$$\mathcal{C}_3 : \textstyle\sum_{k \in \mathcal{S}_m} \|\boldsymbol{w}_k\|_2^2 \leq q_m \quad m = 1, \dots, K_m,$$

$$\mathcal{C}_4 : \textstyle\sum_{k \in \mathcal{S}_m} \boldsymbol{w}_k^H \boldsymbol{R}_{m,p} \boldsymbol{w}_k \leq \tau_p \quad \forall p \in \mathcal{S}_s.$$

Where the utility function represents the weighted sum-rate of the 5G system, with the non-negative factor u_k, denoting the individual weight assigned to each UE, chosen to reflect the different levels of concern about the individual channel gains. A larger gain has a larger weight and vice versa, also constraints $(\mathcal{C}_1 \sim \mathcal{C}_4)$ represent the desired quality of service constraints, with γ_k denoting the QoS threshold for UE *k*; PBS power constraint, MBS power constraint and interference power constraint (i.e., interference generated from MBS to UE *k*) respectively. $\boldsymbol{R}_{m,p} \triangleq \boldsymbol{h}_{m,p}\boldsymbol{h}_{m,p}^H$ is a positive semidefinite (PSD) matrix $(\boldsymbol{R}_{m,p} \geq \boldsymbol{0})$, where $\boldsymbol{h}_{m,p}$ is the channel vector from the MBS to UE *p* and τ_p is the non-negative threshold, which controls the allowable level of interference at UE *k*. Note, that by adding the IC constraint in Eq. (10), it is aimed at shaping the transmission from the MBS, in order to control the significant interference to UEs served by PBS.

Maximizing the weighted sum rate of the 5G heterogeneous network under some given constraints, as expressed in $(\mathcal{C}_1 \sim \mathcal{C}_4)$ is generally regarded as a non-convex, non-deterministic polynomial-time hard (NP-hard) problem because there are no known efficient algorithms that can solve it in polynomial time. However, this intractable problem can be solved by computer algorithms that run in exponential time; such as branch and bound (B&B) algorithms [54], which can give global optimal solutions. B&B algorithms can only be considered for small-scale problems, i.e., problems with very small problem sizes because their running times are exponential functions of their problem sizes. Note, that the problem size in this research work is regarded to be the number of variables and constraints involved in the optimization problem. To pinpoint the actual cause of the non-convexity of the resource allocation optimization problem of Eq. (10), let's analyze each function that makes up the resource allocation problem: firstly, the utility function in Eq. (10) is a concave function that can be maximized, though it depends on the SINRs of UEs in the 5G system. The power constraint functions in $\mathcal{C}_2 \sim \mathcal{C}_3$ together with the MBS interference power constraint function in $\mathcal{C}_4$ are all convex functions. The SINR constraint function in $\mathcal{C}_1$ is a non-convex function of beamforming vectors $\{\boldsymbol{w}_k\}_{k=1}^{K_T}$, which cannot be classified as a semidefinite constraint or second-order cone constraint. To make the constraint convex, $SINR_k \geq \gamma_k$ can be expressed as [55]

$$\frac{1}{\gamma_k}\left|\boldsymbol{h}_{l,k}^{H}\boldsymbol{w}_k\right|^2 \geq \sum_{\substack{p\in\mathcal{S}_l\\ p\neq k}}\left|\boldsymbol{h}_{l,k}^{H}\boldsymbol{w}_p\right|^2 + \sum_{j=1}^{n_{opt}}\sum_{m\in\mathcal{S}_j}\left|\boldsymbol{h}_{j,k}^{H}\boldsymbol{w}_m\right|^2 + \sigma^2 . \qquad (11)$$

It is noted that the absolute values in Eq. (11) make $\boldsymbol{w}_k$ and $e^{j\theta_k}\boldsymbol{w}_k$ equivalent for any common phase rotation $\theta_k \in \mathbb{R}$, hence, this phase ambiguity is exploited to rotate the phase such that $\boldsymbol{h}_{l,k}^{H}\boldsymbol{w}_k$ is real-valued and positive. This insinuates that $\sqrt{\left|\boldsymbol{h}_{l,k}^{H}\boldsymbol{w}_k\right|^2} = \boldsymbol{h}_{l,k}^{H}\boldsymbol{w}_k \geq 0$. Therefore, $SINR_k \geq \gamma_k$ can now be rewritten as

$$\frac{1}{\sqrt{\gamma_k}}\Re\left(\boldsymbol{h}_{l,k}^{H}\boldsymbol{w}_k\right) \geq \sqrt{\sum_{\substack{p\in\mathcal{S}_l\\ p\neq k}}\left|\boldsymbol{h}_{l,k}^{H}\boldsymbol{w}_p\right|^2 + \sum_{j=1}^{n_{opt}}\sum_{m\in\mathcal{S}_j}\left|\boldsymbol{h}_{j,k}^{H}\boldsymbol{w}_m\right|^2 + \sigma^2} \quad . \qquad (12)$$

Where $\Re(\cdot)$ denotes the real part, also, the γ_k value at each UE needs to be fixed. It is assumed that these values are known a *priori* but can be computed as $\gamma_k \triangleq 2^{r_k} - 1$, obtainable from Eq. (9). Therefore, the SINR constraint in Eq. (10) can now be classified as a second-order cone constraint, which is a convex type constraint [56].

One of the focus of this section is to produce approximate solutions that are feasible in practice for large-scale problems. Consequently, the non-convex problem will be solved using the convex heuristics approach.

The RA problem in Eq. (10) is centralized and the optimization variable is the transmit beamformers. Note that the properties of these transmit beamformers include both the spatial characteristic and the corresponding transmission powers. Recall that the RA aims to allocate powers and spatial directions to UEs in the 5G system, to maximize the system sum rate while satisfying power, QoS, and interference constraints. Having said that, Eq. (10) is readily split into two sub-problems. The first problem is formulated as a spatial direction allocation problem, while the second problem is formulated as a power allocation problem. The former needs to be solved centrally while the latter will be solved in a decentralized manner. This technically means that the RA problem in Eq. (10) is decomposed into two subproblems, giving more freedom to each BS to determine the performance level for each served UE.

3.3 Spatial Direction Allocation Problem

The spatial direction allocation problem is expressed as

$$\tilde{\boldsymbol{w}}_k = \underset{\{\boldsymbol{w}_k\}_{k=1}^{K_r}}{\operatorname{argmax}} \sum_{k=1}^{K_r} u_k r_k(\{\boldsymbol{w}_k\}),$$

$$\text{subject to} \quad \mathcal{C}_1: \frac{1}{\sqrt{\gamma_k}} \Re\left(\boldsymbol{h}_{l,k}^H \boldsymbol{w}_k\right) \geq \Gamma_k,$$

$$\mathcal{C}_2 \sim \mathcal{C}_4 \text{ in } (10), \tag{13}$$

$$\mathcal{C}_5: \|\boldsymbol{w}_k\|_2^2 = 1 \quad k = 1, \ldots, K_r,$$

where $\Gamma_k = \sqrt{\sum_{\substack{p \in \mathcal{S}_l \\ p \neq k}} \left|\boldsymbol{h}_{l,k}^H \boldsymbol{w}_p\right|^2 + \sum_{j=1}^{n_{opt}} \sum_{m \in \mathcal{S}_j} \left|\boldsymbol{h}_{j,k}^H \boldsymbol{w}_m\right|^2 + \sigma^2}$. To solve Eq. (13) efficiently, SeDumi [57], which is a general-purpose implementation of the interior point method, with CVX [58], which provides a MatLab-based modeling platform for it, were adopted and utilized to provide values for the unit-norm beamformers or spatial directions. Therefore, the unit-norm beamformers or spatial directions of the system are denoted as $\{\tilde{\boldsymbol{w}}_1, \ldots, \tilde{\boldsymbol{w}}_{K_r}\}$.

The next Section presents the design of optimal transmit power allocated to each UE in each cell to improve UE performance and maximize the sum rate of a 5G heterogeneous network.

3.4 Power Allocation Problem

The major interference problem has been tackled in the previous section by designing unit-norm beamformers $\{\tilde{\boldsymbol{w}}_1, \ldots, \tilde{\boldsymbol{w}}_{K_r}\}$ that will spatially separate data symbols when transmitting to UEs. Any negligible interference in the system will be modeled as part of the background noise. What is left to be done is to select the power allocation coefficient $\{p_k\} \forall k \in \mathcal{S}_j$ which will act as the optimum scale factor for each spatial direction to maximize the SE of the system as well as satisfy each UE with a minimum performance level. The power resource allocation problem is hereby formulated as

$$\underset{\{p_k\}\forall k \in \mathcal{S}_j}{\text{maximize}} \quad \sum_{k \in \mathcal{S}_j} \log_2\left(1 + p_k \frac{\left|\boldsymbol{h}_{j,k}^H \widetilde{\boldsymbol{w}}_k\right|^2}{\sigma^2}\right),$$

$$\text{subject to } \textstyle\sum_{k \in \mathcal{S}_j} p_k \leq q_j \,, \tag{14}$$

$$\log_2\left(1 + p_k \frac{\left|\boldsymbol{h}_{j,k}^H \widetilde{\boldsymbol{w}}_k\right|^2}{\sigma^2}\right) \geq R_k \quad \forall k \in \mathcal{S}_j,$$

$$p_k \geq 0 \;\; \forall k \in \mathcal{S}_j.$$

Where R_k denotes the minimum required data rate for UE k to have a good quality of experience (QoE). One can easily observe that the power RA problem in Eq. (14) is a convex optimization problem, because the utility function is concave while the constraint functions are: convex function, concave function, and concave function respectively. Hence, the global power solution was obtained efficiently using CVX, a package for specifying and solving convex programs. For fairness in this power RA formulation to be achieved, this constraint $\log_2\left(1 + p_k \frac{\left|\boldsymbol{h}_{j,k}^H \widetilde{\boldsymbol{w}}_k\right|^2}{\sigma^2}\right) \geq R_k$ needs to be active. In some cases, it is not but it all depends on how large this threshold R_k is.

The resource allocation procedure in this section is summarized using Algorithm 3.1.

3.5 Algorithm

Algorithm 3.1 *Allocation of spatial directions and powers for each UE in heterogeneous 5G network*

Input and variables

$\mathcal{S}_j$: set of UEs served by BS_j;

K : total number of UEs in each cell;

procedure

1: **for** UEs $\in \mathcal{S}_j$ i.e., k = 1 to K **do**

2: compute the unit-norm beamformers $\tilde{\boldsymbol{w}}_k$ using Eq. (13);

3: compute $\{p_k\}\forall k \in \mathcal{S}_j$ from using Eq. (14);

4: **end for**

BS_j Transmit $\boldsymbol{x}_j = \sum_{k\in\mathcal{S}_j} \sqrt{p_k}\tilde{\boldsymbol{w}}_k s_k$.

3.6 Results Obtained

a) Results obtained from our published work

One of the expected project outcomes for this research is to train postgraduate students in the area of current and future wireless communication technology. In this regard, one of the master's students Ms. Chiamaka Blossom Nwabanne was given a project topic in line with this research project. She developed a thesis under my supervision which was entitled "Improving the Spectral Efficiency of a 5G Massive MIMO system using Beamforming." From this work, we were able to publish an article in the UNIZIK Journal of Engineering and Applied Sciences (2023), https://journals.unizik.edu.ng/index.php/ujeas. The title of the published work is "Improving the Spectral Efficiency of an Uplink 5G Massive MIMO System Using Convex Optimization Approach". This article was made possible as a result of this research. Notable results presented in the article include:

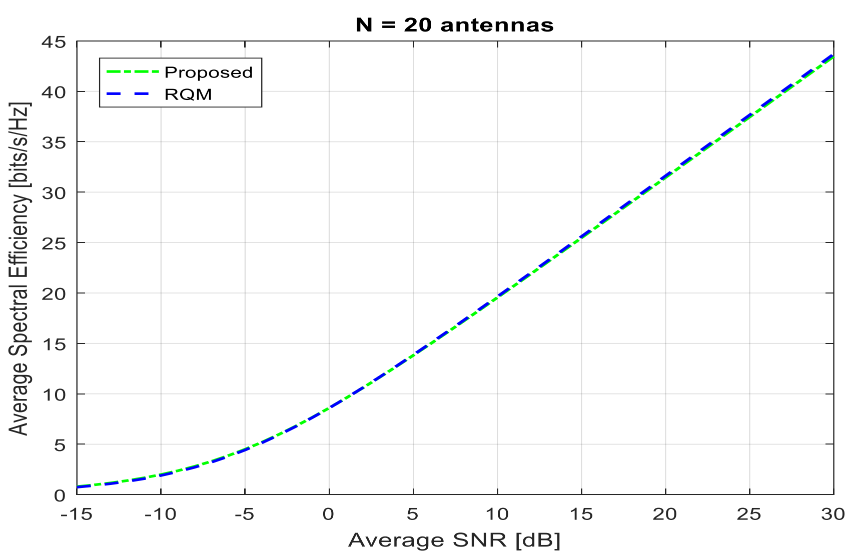

Fig. 3.1: Average Spectral efficiencies achievable at different SNR for N=20, M=4

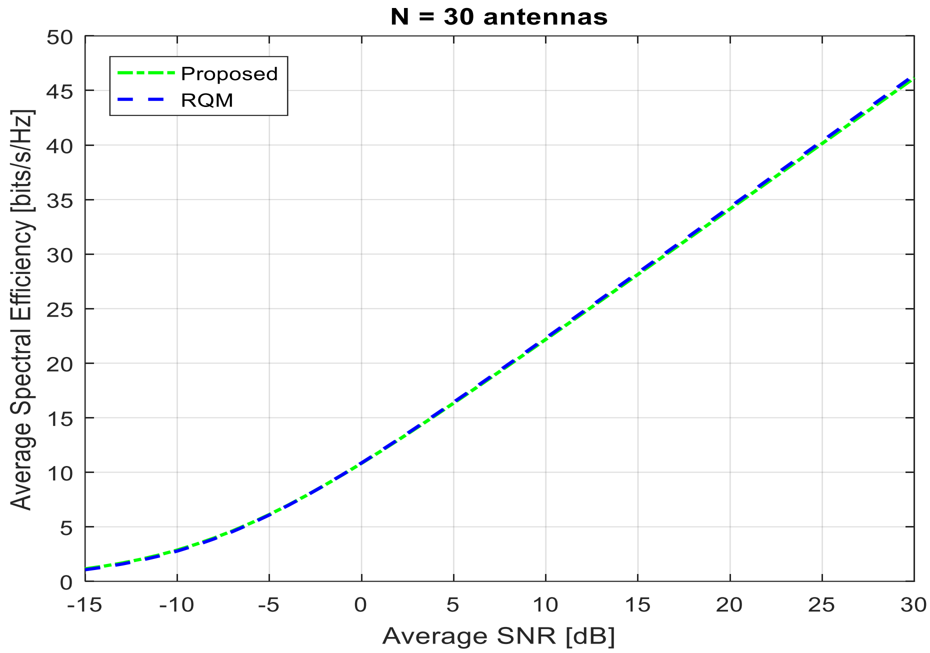

Fig. 3.2: Average Spectral efficiencies achievable at different SNR for N=30, M=4

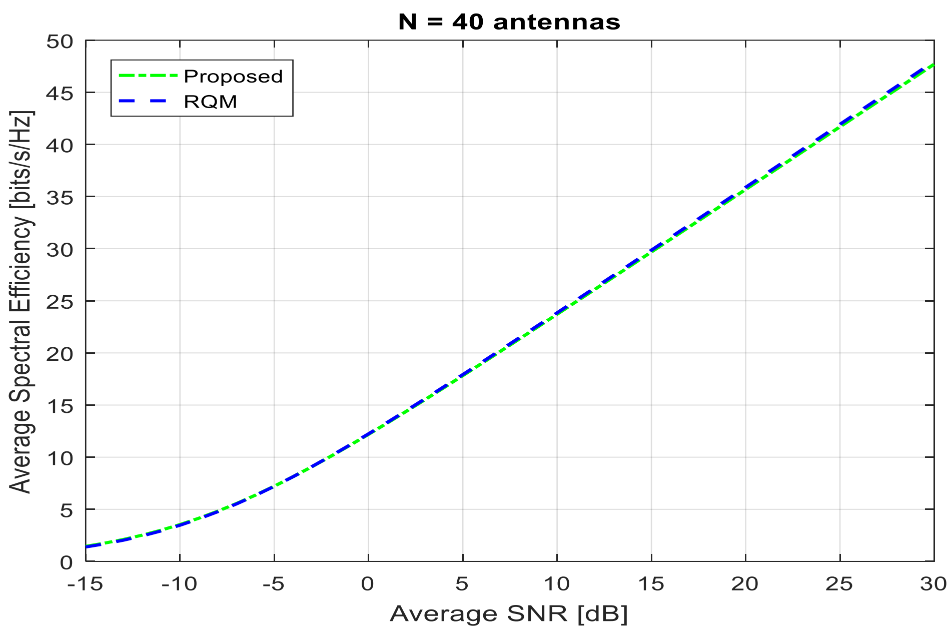

Fig. 3.3: Average Spectral efficiencies achievable at different SNR for N=40, M=4

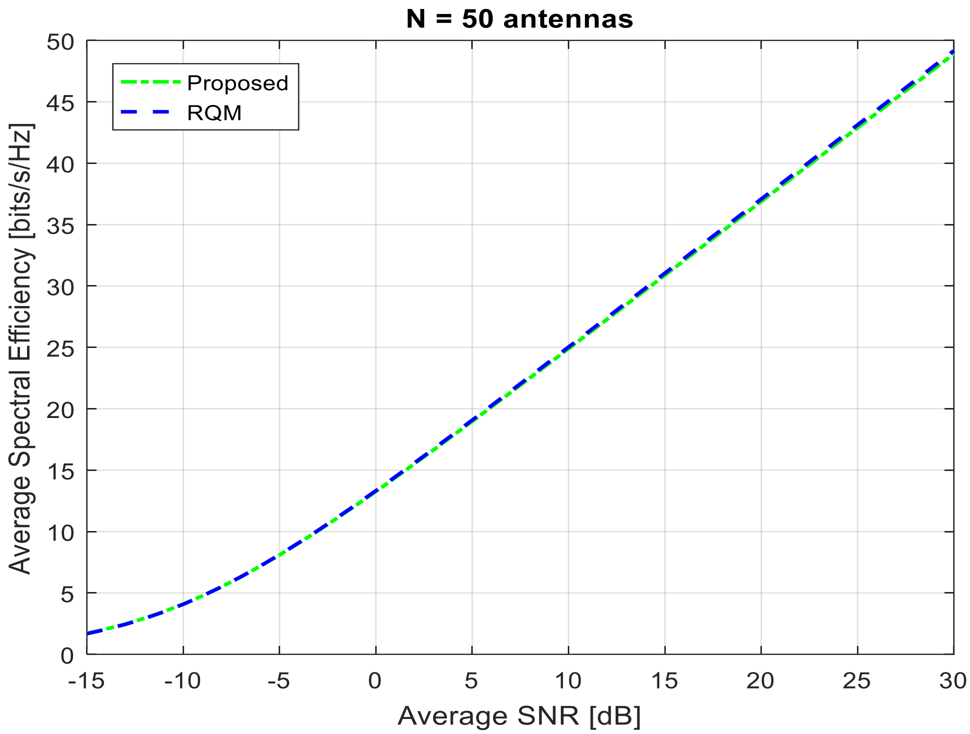

Fig. 3.4: Average Spectral efficiencies achievable at different SNR for N=50, M=4

In Fig. 3.1, the average cell spectral efficiency achievable at SNR = 30dB, N = 20, and M = 4 is approximately 44 bits/s/Hz for both the proposed and the Rayleigh Quotient Method (RQM) which is an analytical method used to obtain the optimal beamformers in the uplink of a cell. This also proves that the method proposed in this work is optimal since similar values were obtained by the proposed method and the RQM despite the proposed method being a numerical method.

Using the same parameters (M =4, and SNR = 30dB), Figures 3.2, 3.3, and 3.4 respectively show that slight improvements were achieved in the cell spectral efficiency (46bits/s/Hz, 47.5bits/s/Hz, and 49bits/s/Hz) when the base station receive antennas N were increased. This also shows that for a meaningful improvement in the spectral efficiency of a cell, the UE component needs to increase as well as the base station receive antennas. For more explanation on this, see Fig. 3.5 and Fig.3.6 respectively.

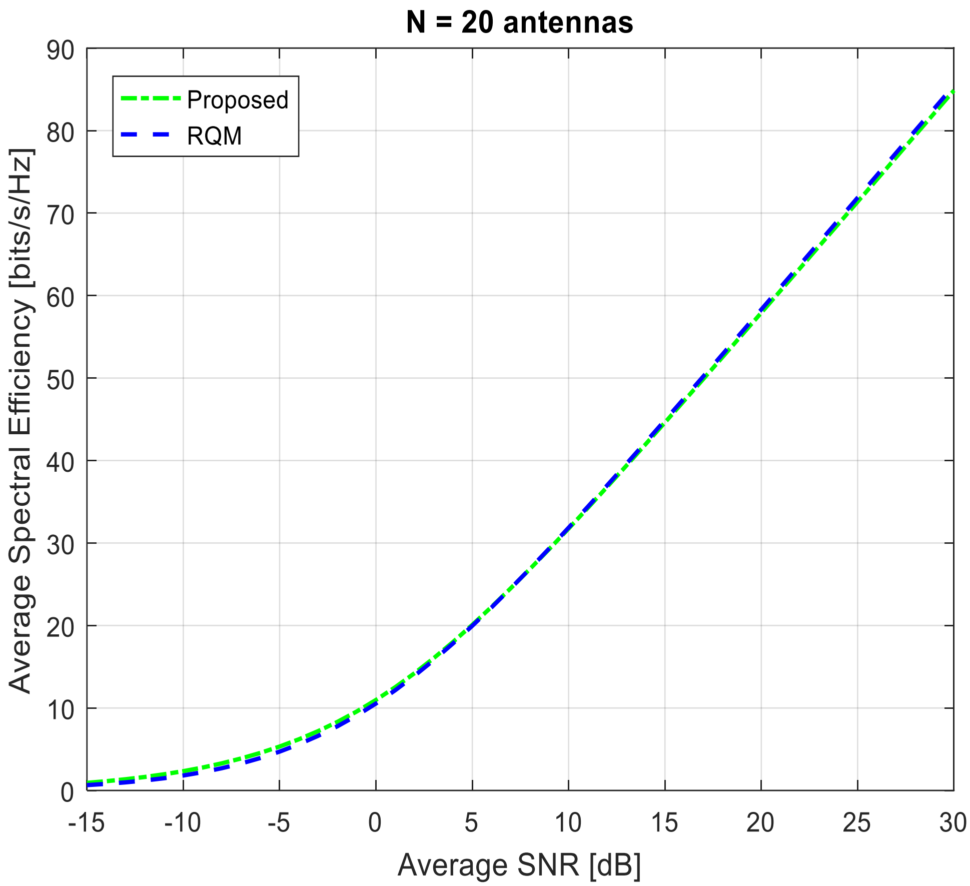

Fig. 3.5: Average Spectral efficiencies achievable at different SNR for N=20, M=9

In Fig. 3.5, the average cell spectral efficiency is improved to 85 bits/s/Hz based on the following parameters (SNR = 30 dB, N =20, M = 9). When compared to Fig. 3.1 which has similar parameters except M = 4. One can see that the difference in the spectral efficiency achieved in both figures at SNR = 30dB is 41 bits/s/Hz.

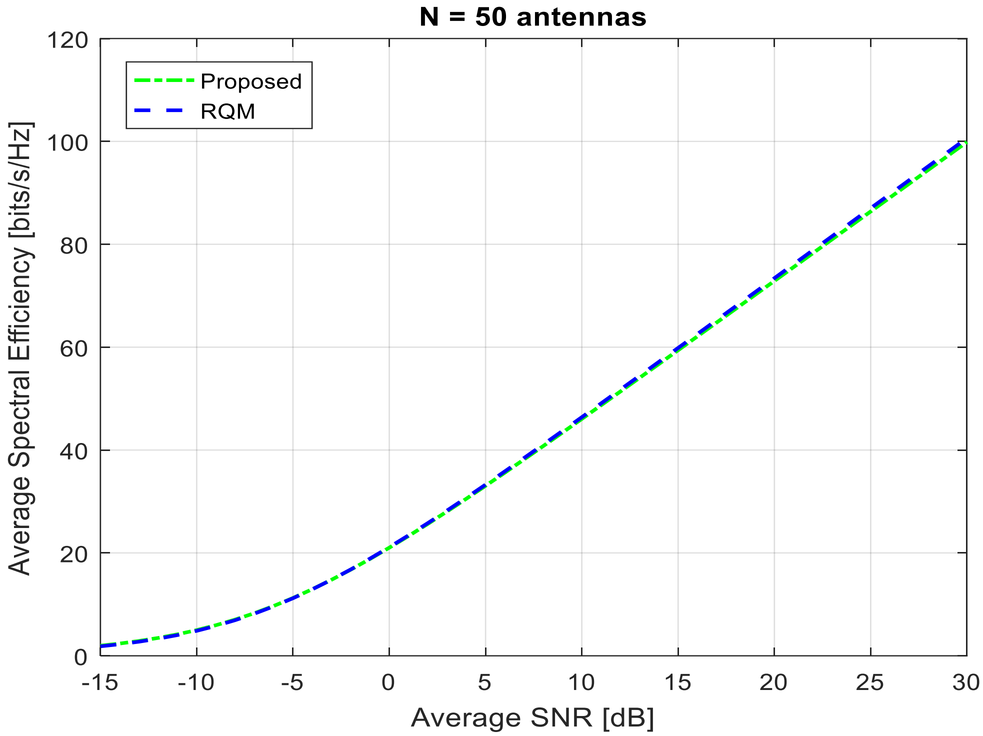

Fig. 3.6: Average Spectral efficiencies achievable at different SNR for N=50, m=9

In Fig. 3.6, the average cell spectral efficiency achievable at SNR = 30dB is improved to 100bits/s/Hz. When compared to Fig. 3.4 at the same SNR = 30dB, the same receive antenna elements, but at a lesser number of UEs, one can see that the spectral efficiency achieved for that figure reduced to 49 bits/s/Hz. So, the gain in spectral efficiency when comparing Fig. 3.6 to Fig. 3.4 stood at 51 bits/s/Hz.

b) Results obtained from our published paper in the Journal of Inventive Engineering and Technology (JIET)

The title of the submitted paper is “User-centric Based Clustering Scheme and Resource Allocation for Inter-cell Interference Mitigation in 5G Heterogeneous Networks.” Notable results presented in the journal paper include:

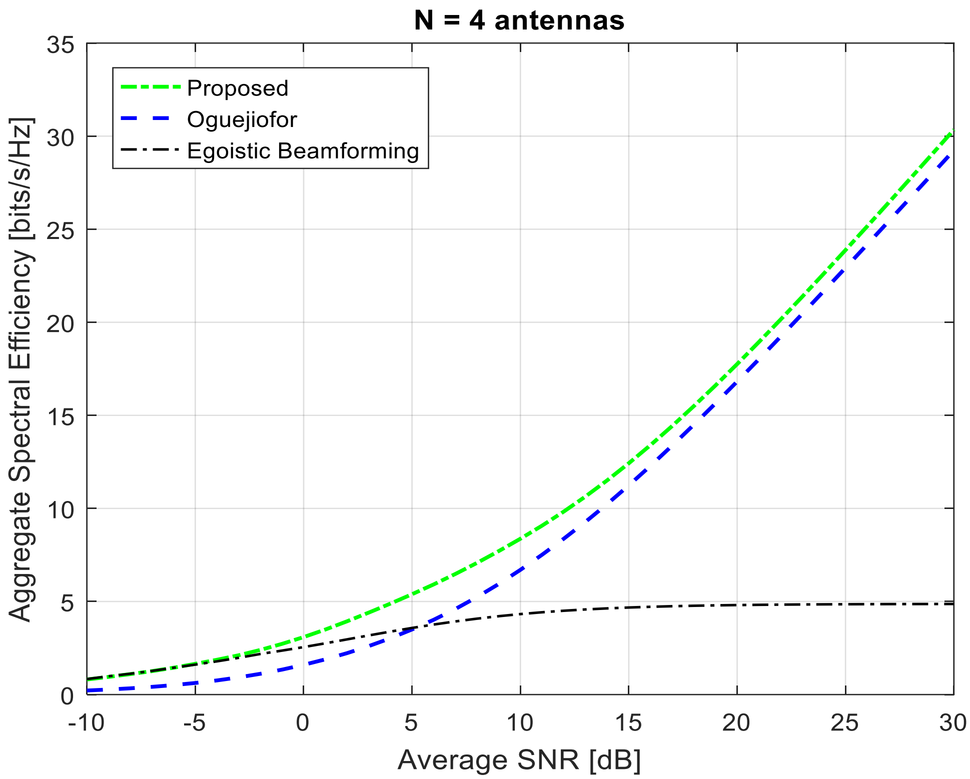

Fig 3.7: Aggregate Spectral Efficiency as a function of SNR for different beamformers

In Fig. 3.7, the proposed method outperforms methods used by Oguejiofor *et al* and the Egoistic beamforming method. The Egoistic beamforming method is a method whose design doesn't consider interference from other cells. The method is more interested in designing beamformers for UEs in each cell without considering interference from other cells. This method as can be seen cannot compete with the proposed method when applied to a 5G system where inter-cell interference is a factor because universal frequency is being utilized.

The theoretical minimum achievable spectral efficiency for a 5G system is 30 bits/s/Hz based on 3GPP technical specifications. If you are using this value as a baseline, then it will take the following parameters (Kr=4, N=4, SNR = 30dB) for the proposed method to actualize it. The egoistic beamforming method cannot achieve that based on the same parameters, while it will take the Oguejiofor *et al* method a higher SNR to achieve that.

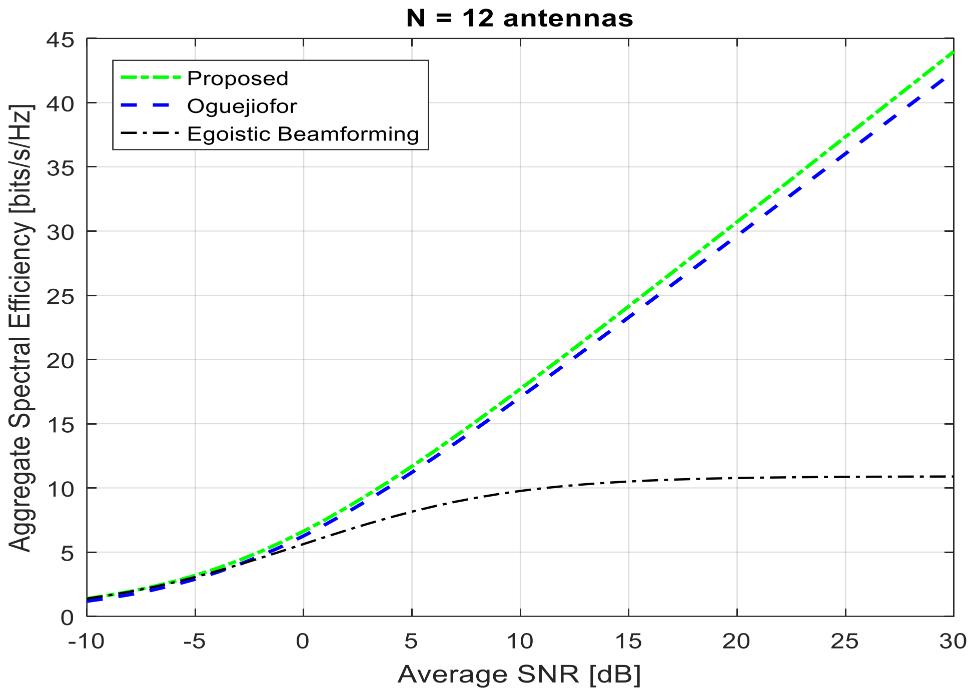

Fig. 3.8: Aggregate Spectral efficiencies achievable at different SNR for *N*=12, *Kr*=4.

In Fig 3.8, The proposed method at *SNR* = 30dB was able to achieve a spectral efficiency of 43 bit/s/Hz, while the Oguejiofor *et al* method also surpassed the 30 bit/s/Hz at *SNR*=30dB. At *SNR* = 30dB for Fig. 3.7 and Fig. 3.8 respectively, one can see clearly that the proposed method achieved an improved spectral efficiency of 13bits/s/Hz. This is due to an increase in the number of transmit antennas in each BS in each cell. The Egoistic beamforming method should not be applied to a 5G system that wants to improve its spectral efficiency because it will be greatly affected by inter-cell interference due to the adoption of universal frequency re-use by 5G systems.

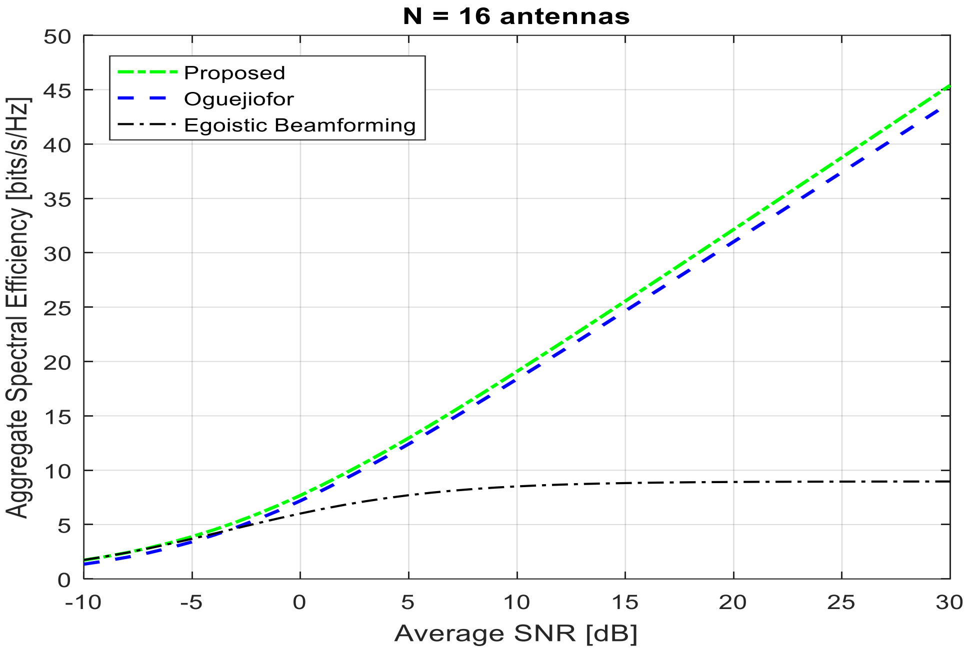

Fig. 3.9: Aggregate Spectral efficiencies achievable at different SNR for *N*=16, *Kr*=4

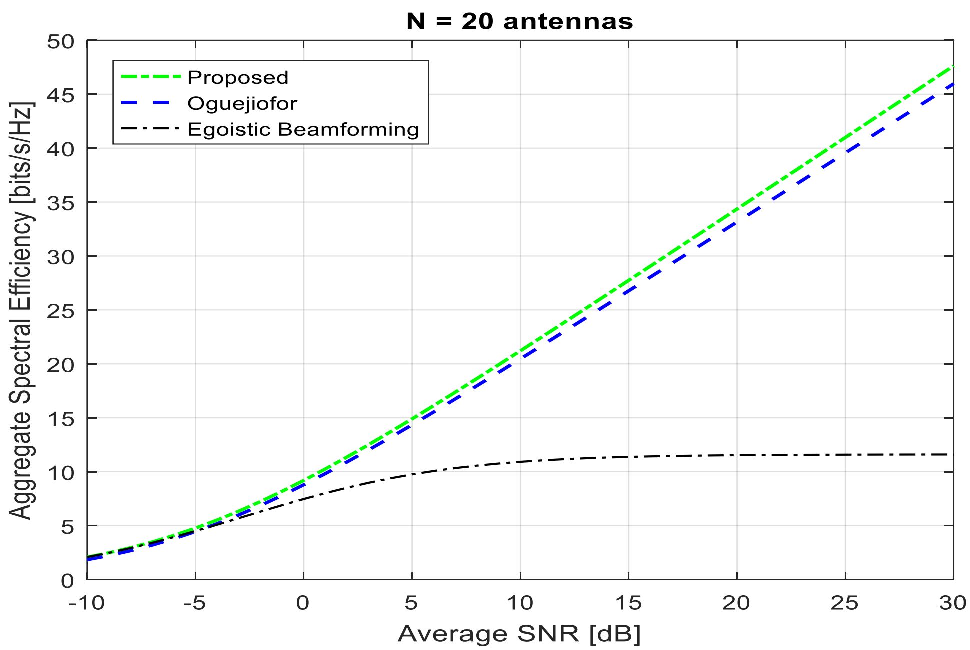

Fig. 3.10: Aggregate Spectral efficiencies achievable at different *SNR* for *N*=20, *Kr*=4

In Fig. 3.9 and Fig. 3.10 respectively, at SNR =30dB, the achievable spectral efficiency in the system by the proposed method is 45 bits/s/Hz and 48 bits/s/Hz. The improved spectral efficiency achieved is due to the optimally coordinated beamformers designed by the proposed method which helps the transmit antenna to focus the desired signal energy to the desired UE.

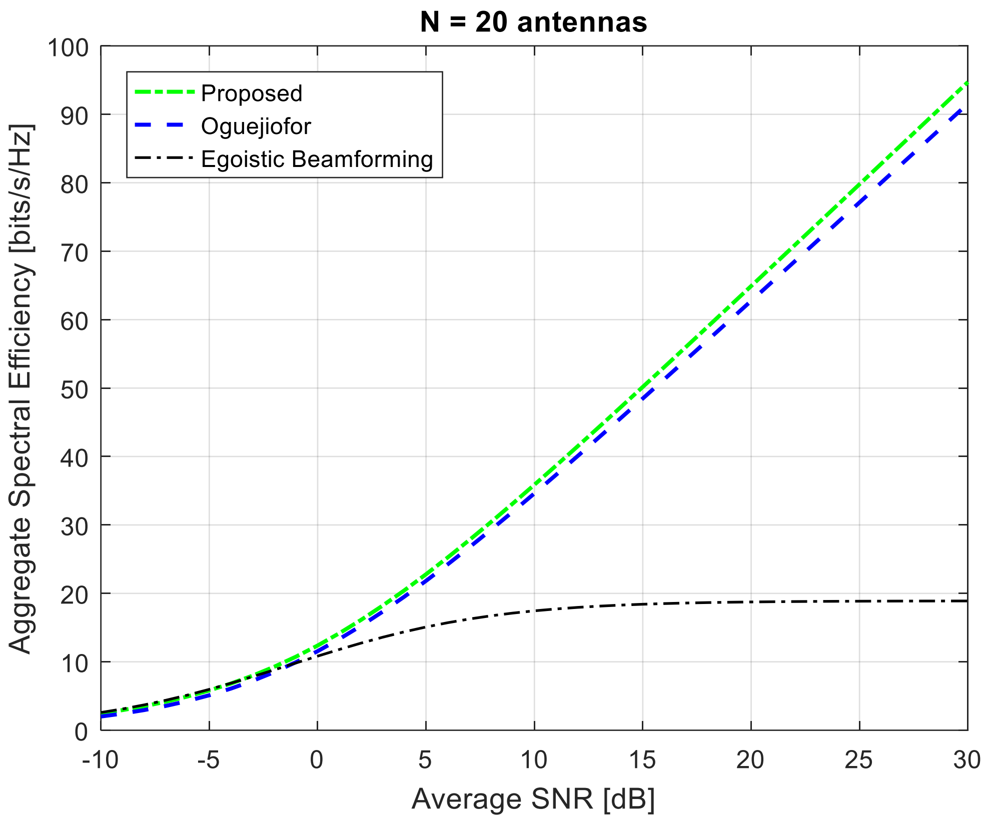

Fig. 3.11: Aggregate Spectral efficiencies achievable at different *SNR* for *N*=20, *Kr*=9.

In Fig. 3.11, the aggregate spectral efficiency achievable for the proposed method is 95 bits/s/Hz. When compared to the aggregate spectral efficiency achievable for the proposed method in Fig. 3.10, which has the following parameters (*N* =20, *Kr* =4), one can see that at SNR = 30 dB, the achievable aggregate spectral efficiency is at 48 bit/s/Hz. The aggregate spectral efficiency in Fig. 3.11 is improved by 47bits/s/Hz to that achievable in Fig 3.10 at *SNR* = 30dB.

What this means is that as the number of UEs increases in the system, together with the transmit antenna at each base station, the aggregate spectral efficiency of that system must increase when coordinated beamforming methods like the one proposed in this work are utilized at the base stations for precoding of signals before downlink transmission.

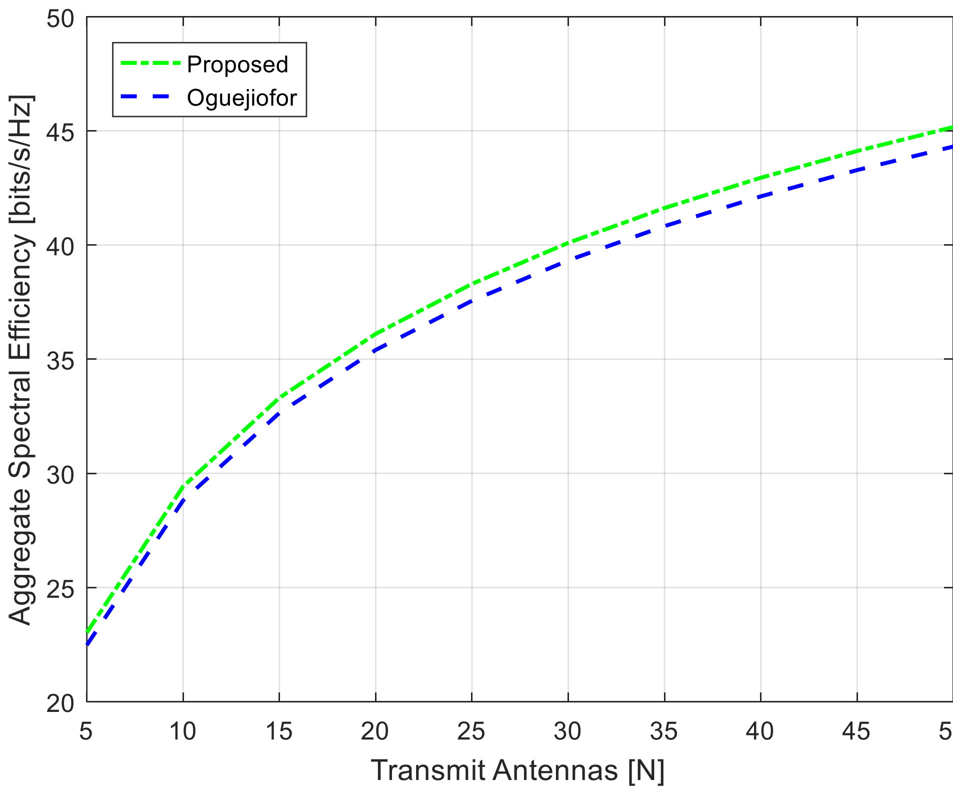

Fig. 3.12: Aggregate spectral efficiency at different transmit antenna for *SNR* = 10dB

In Fig 3.12, the plot of the aggregate spectral efficiencies of the system as a function of the number of transmit antennas in base stations shows that at low SNR = 10dB, for 20 transmit antennas, the spectral efficiency achievable by the proposed method is approximately 37 bits/s/Hz, while that of oguejiofor *et al* beamforming method is approximately 36 bits/s/Hz. This is quite similar to the figures obtained in Fig. 3.11 under SNR = 10dB. However, it was observed that to achieve a minimum spectral efficiency of 30 bit/s/Hz which is the minimum requirement for a 5G system by 3GPP 5G technical specifications, for a low SNR =10dB, the number of transmit antennas needed at the base stations must be greater than 10.

SECTION FOUR: STAGE FOUR DELIVERABLE REPORTS

4.1 Introduction

Some discussions are relevant to the main focus of this report which is the design and development of a transmitter incorporating a multi-antenna system. These discussions are necessary because they provide clarification, justification, or motivation behind factors considered while trying to design and implement the stage four prototype. Henceforth we termed these discussions as “REMARK.”

4.1.1 REMARK 1: Resource Block

In the context of wireless communication systems, a resource block (RB) refers to a specific block of time-frequency resources allocated for data transmission in a cellular network. It is primarily used in the Long-Term Evolution (LTE) and 5G wireless standards. In both LTE and 5G, the available frequency band is divided into small subcarriers, and the transmission time is divided into time slots, these subcarriers and time slots are considered to form resource blocks. Each resource block consists of a separate number of subcarriers in the frequency domain and a specific number of time slots in the time domain. By dividing the available spectrum and time slots into resource blocks, cellular networks can effectively allocate resources to multiple users simultaneously using orthogonal frequency division multiple access (OFDMA), allowing for concurrent data transmission and reception. However, in OFDMA, the challenge is the inter-cell interference. In OFDMA, inter-cell interference can be seen as a collision between resource blocks. Resource block collision can occur when neighboring/adjacent cells use the same resource blocks for transmission leading to inter-cell/co-channel interference which is capable of degrading the overall system capacity.

Part of our effort in this research is to prevent or curb resource block collision.

4.1.2 REMARK 2: Factors that Influence the Design and Implementation of the Prototypes

To show that the algorithm devised in the stage three deliverable report can provide solutions to cochannel/inter-cell interference in 5G networks and other wireless networks by avoiding resource block collision using the proposed prototypes. We considered a lot of factors/questions like:

a) Which Radio frequency band are we going to adopt where the proposed prototype devices can operate?
b) The Radio frequency band must be capable of being re-used by other network devices to fulfill the universal frequency reuse condition and bring about high spectral efficiency.
c) The Radio frequency band must be unlicensed because the scope of this research doesn't include identity authentication and core signaling security. Furthermore, the more interference existing in the band the better way to validate the devised algorithm.

The answers to the above questions and considerations made us now to settle for the following:

d) To implement the proposed prototype, we will be adopting the 5G S-band. Because most parts of this band are unlicensed, it can be reused as well by other network devices. However, it will create issues like a lot of co-channel interference because it is an unlicensed Radiofrequency band. We are aware that most cellular networks don't use S-Band partly because it is an unlicensed band.
e) So, based on factors (a) to (d), our goal remains the same which is to design and develop a multi-antenna system with an embedded transmitter that will operate under universal frequency reuse without being affected much by cochannel/ inter-cell interference due to the algorithm controlling it.

Altogether we developed prototypes comprising the following:

1. Two (2) units of base stations i.e. (multi-antenna systems with embedded transmitters for the transmission of Radiofrequency signals).
2. Two (2) units of user equipment or receivers for reception of the Radiofrequency signals.
3. One (1) unit of an external power system that provides power for the base stations.

4. One (1) unit of a network visualizer device that provides graphical illustrations of different resource blocks (see remark 1) or channels and the number of user equipment connected to it.

We aim to utilize the proposed prototypes to show how the devised algorithm and some coding can help curb co-channel/inter-cell interference caused by resource block collision in a wireless network.

4.2 Design and Development of Transmitter Incorporating Multi-Antenna System

In this section, we described how the multi-antenna systems with embedded transmitters were designed and developed.

4.2.1 Materials

Some of the materials (hardware and software) used to achieve the prototypes include:

- ✓ ISM43340 Chipset
- ✓ Flame retardant (FR-4)
- ✓ Radio Frequency Spectrum Analyzer
- ✓ Laptop with Windows 10
- ✓ PCB Printer
- ✓ PCB CAD Designer
- ✓ Meandered Planer Inverted-F Antenna
- ✓ Software Define Radio
- ✓ Arduino Integrated Development Environment
- ✓ C++
- ✓ ESP8266 Micro chipset
- ✓ Custom PCB

ISM43340 Chipset: It is a module that operates in the 2.4 & and 5.0 GHz spectrum. The wireless fidelity module's hardware consists of an ARM Cortex M4 host processor, Cypress CYW43340 Dual-Band (2.4 GHz / 5 GHz) 802.11 a/b/g/n MAC/Baseband/Radio with Integrated Bluetooth (BT)/ Bluetooth Low Energy (BLE) 5.0.

Software-Defined Radio: Software-defined radio (SDR) is a radio communication system where components that conventionally would have been implemented in analog hardware (e.g., mixers, filters, amplifiers, modulators/demodulators, detectors, etc.) are instead implemented using software on a personal computer or embedded system.

Arduino Integrated Development Environment: It is an official software introduced by Arduino. cc, which is mainly used for writing, compiling, and uploading code in almost all Arduino modules/boards. The platform is an Open-source electronic prototyping platform enabling users to create interactive electronic objects.

EPS 8266 Microchipset: The ESP8266 is a low-cost wireless fidelity microchip, with built-in Transmission control protocol/internet protocol (TCP/IP) networking software, and microcontroller capability, produced by Espressif Systems. The module allows microcontrollers to connect to a wireless network and make simple TCP/IP connections using Hayes-style commands.

Custom PCB (Printed Circuit Board): It is a circuit board that is specifically designed and fabricated for a particular electronic device or project, rather than using a standard off-the-shelf board.

4.2.2 Methodology

We adapted the ISM 43340 chipset which has a transceiver (transmitter and receiver) module through coding to suit our design, which is a transmitter incorporating a multi-antenna system. Note that the ISM 43340 hardware module does not natively support multiple antenna elements. However, we were able to tweak this to develop a transmitter incorporating a multi-antenna system by utilizing a custom PCB design, and, also by leveraging on the ISM43340 radio which operates as an SDR, which gives us an avenue to use software to manipulate what the functionality of the module. Furthermore, Arduino IDE grants us the additional ability to control the ISM 43340 module through coding using C++ to achieve the functionality we want.

Getting the ISM 43340 to function as a transmitter only, was achieved through coding using C++ as the programming language. The codes written for that functionality were burned into the ISM 43340 module through the flash port or USB interface. see Fig, 4.1 for the block diagram of the ISM 43340 chipset.

The flash port is a port used for programming the internal flash memory of the chip. Flash memory is a type of non-volatile memory that can be electrically erased and reprogrammed. One can use any of the programming interfaces while programming such as the inter-integrated circuit (I2C), serial peripheral interface (SPI), etc. We utilized these programming interfaces to burn software codes onto the radio chip's internal flash memory, enabling the chip to perform the function we wanted such as how the transmitter will send signals to the antennas. Note that the flash port will work with different communication mediums as shown in Fig. 4.1.

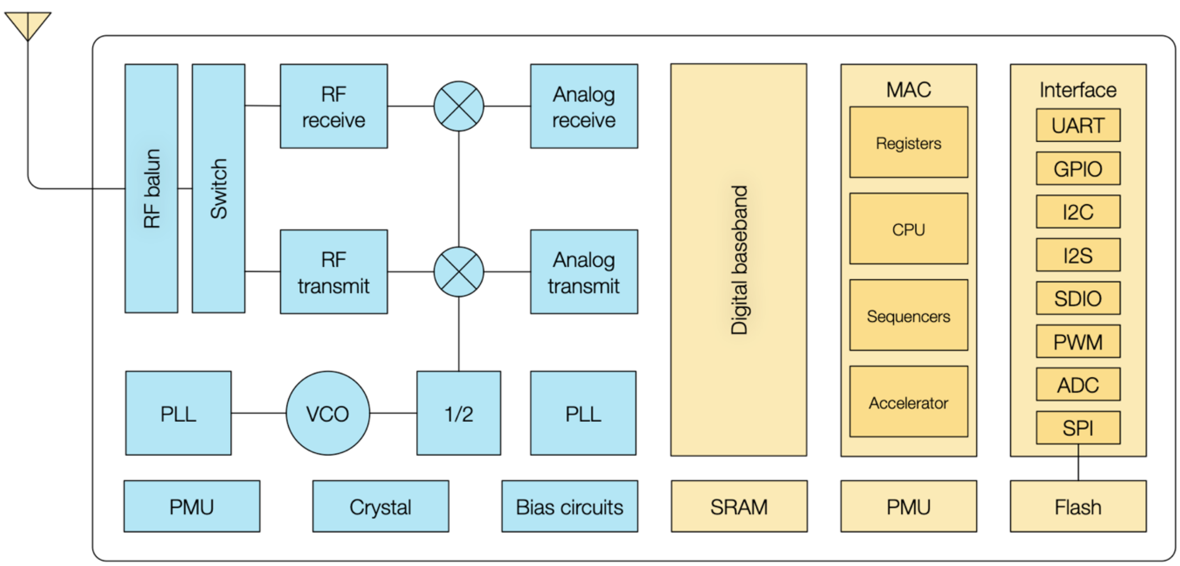

Figure 4.1 Block diagram of ISM43340 Chipset

During Execution, the central processing unit (CPU) sends control signals, such that the program code will be moved to the static random-access memory (SRAM) and then will start executing the codes line by line. For example, during transmission of RF signals, the RF transmit block will be activated and programs written for transmission will be executed in line with the code written for it. During reception, the RF-Receive block will be activated, the signal received is analog, hence it will first be converted to digital using an analog-to-digital converter (ADC). Afterwards, it will be forwarded to the CPU which will now hold the instruction in a particular register, etc.

The schematic diagram of a single ISM 43340 Chipset before adaptation to our design using coding is shown in Fig. 4.2

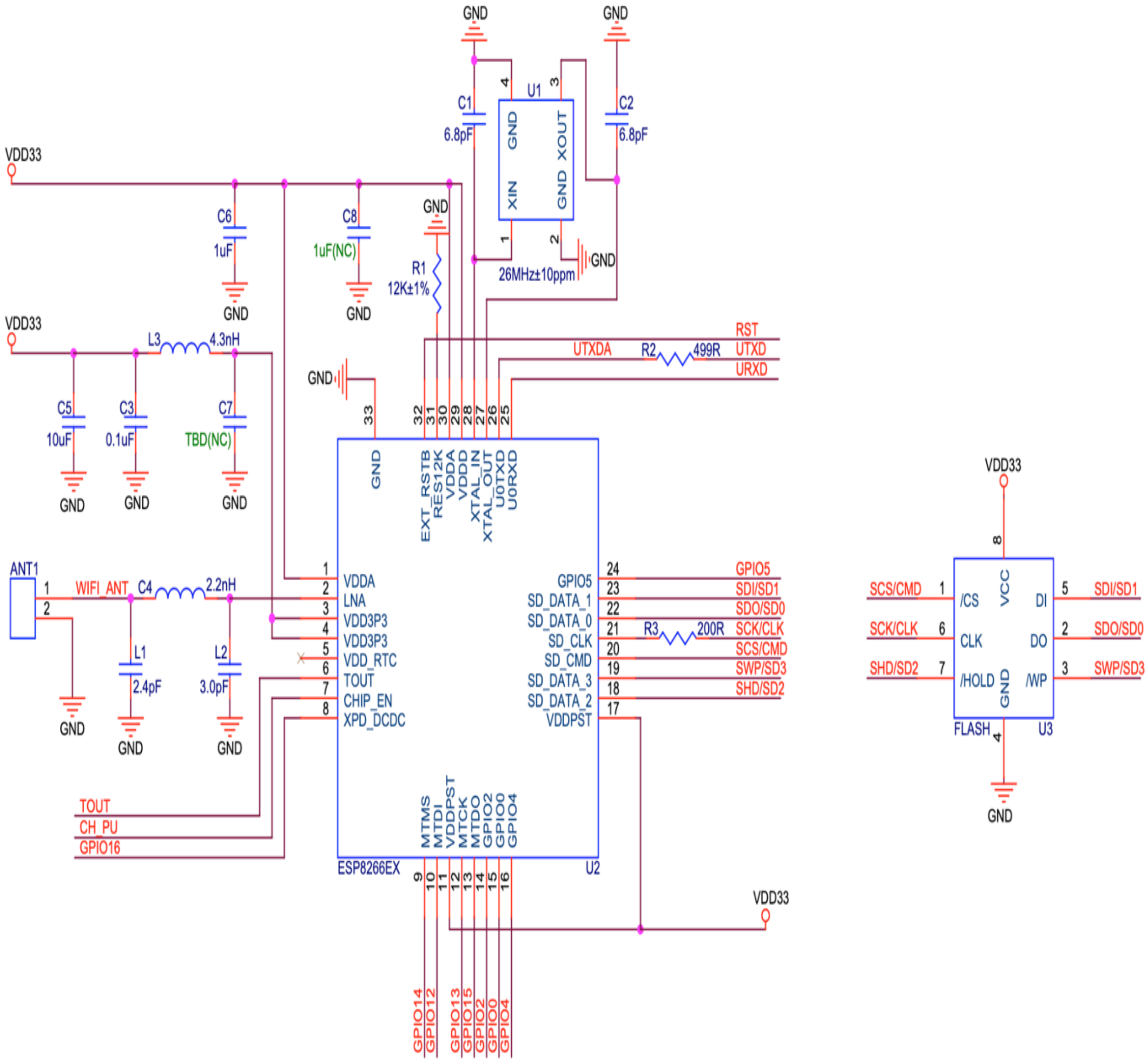

Figure 4.2 Schematic Circuit Diagram of a Single ISM 43340

4.2.2.1 Design of a Custom PCB for the Development of the Transmitter Incorporating Multi-Antenna System

In this subsection, we show step by step procedure on how the custom PCB for the development of the multi-antenna system with embedded transmitters was designed

1) Schematic Design: This is the first step we undertook to create a schematic diagram of the circuit. This diagram shows interconnections between the components and their functions. Please see Fig. 4.3 for the schematic diagram of the design of the multi-antenna system with embedded transmitters
2) PCB Layout Design: In this step, we design the physical layout of the PCB. It involves placing the components on the board and routing the electrical connection between them. Eagle PCB design software was utilized for this purpose.
3) Component Selection: In this step, we chose the various components that will be used in the circuit, including the ISM 43340 chipsets, the power switch, the cooling fan, the internal power that supplies the needed voltage, etc. These were soldered onto the PCB after the manufacturing stage.

4) PCB Manufacturing: In this step, the PCB was manufactured according to the design specifications. This step involved processes such as etching, drilling, and solder masking.

5) Assembly: In this step, we soldered the components needed for the development of the multiantenna system with embedded transmitters as stated in step 3.

6) Testing: we performed testing to ensure that the circuit performed as expected. It was at this point that we noticed that the internal power supply wouldn’t be enough to power the multi-antenna system and it gave rise to the development of an external power supply circuit.

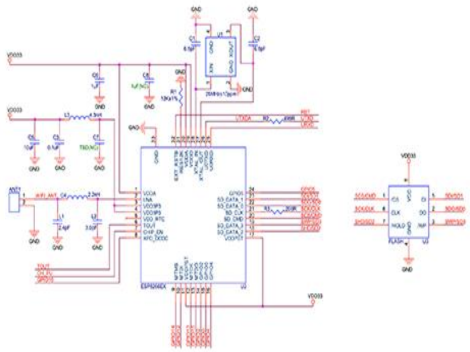
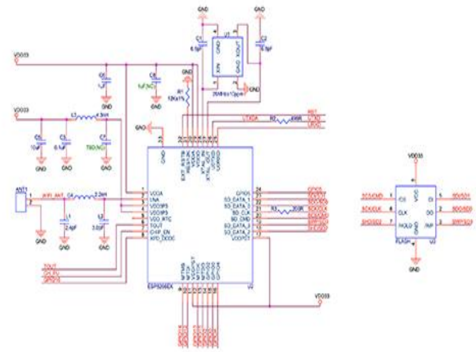
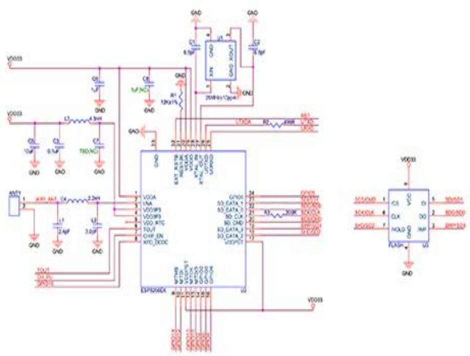
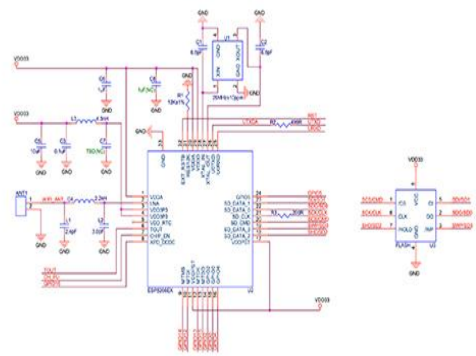
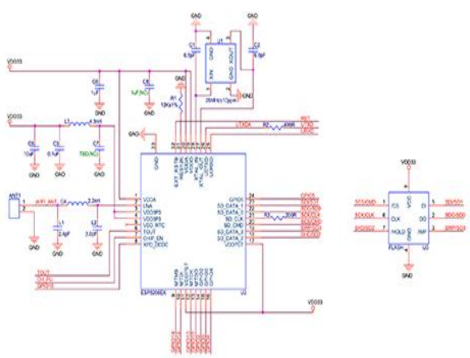
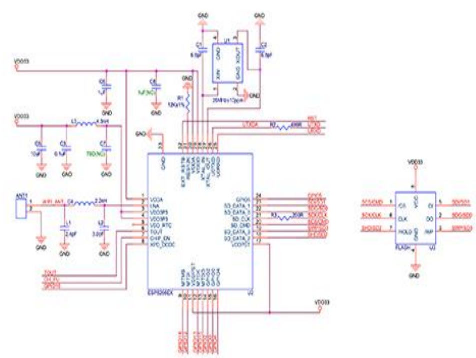
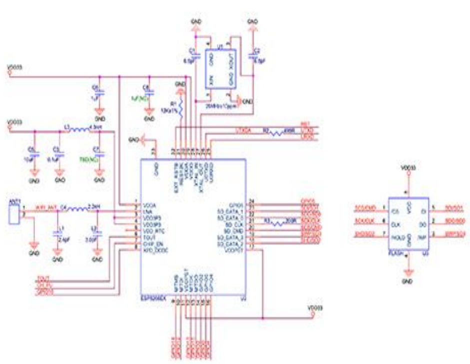
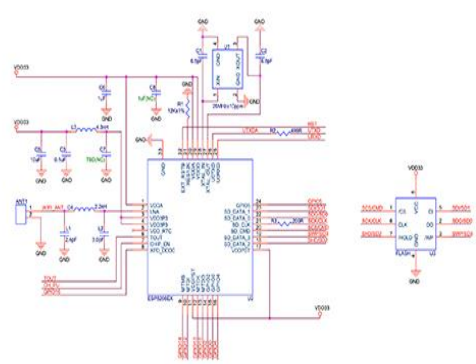

Figure 4.3 Schematic Diagram for the design of the multi-antenna system with transmitters

4.2.2.2 Multi-Antenna System Design Implementation

The antenna array (multi-antenna elements) was printed on a flame retardant 4 (FR-4) dielectric board with a size of 140 × 70 × 0.8 mm^3. The antennas are evenly arranged on both sides of the printed circuit board (PCB).

Each of the multi-antenna systems designed in this work contains a total of two (8x1) antenna elements, making it a total of 16 antenna elements per multi-antenna system. The two symmetrical blocks of antenna elements on each side of the metal backplane had a spacing of 13 mm, and the distance between the block of antenna elements on both sides was 33 mm from the edge of the backplane. The selection of an antenna depends on the application, the available board size, cost, Radio frequency range, and directivity. Antenna design and Radiofrequency layout are critical in any wireless system that transmits and receives electromagnetic radiation in free space. The wireless range that user equipment gets out of a Radiofrequency product with a current-limited power source such as a coin-cell battery depends greatly on the antenna design, the enclosure, and a good PCB layout. The antenna structure utilized in this project is a meandered planar inverted-F antenna (mPIFA) loaded with slots, as shown in Figure 4.4. The antenna is resonant at a quarter-wavelength (thus reducing the required space needed on the device), and also typically has good specific absorption rate (SAR) properties. This antenna resembles an inverted F, which explains the mPIFA name. The mPIFA antenna has the advantages of low profile, easy matching, etc., and does not require additional headroom. If the mPIFA is of length $L1$, width $L2$ and shorting pin of width W, the resonant frequency of the PIFA depends on W.

If $W = L2$, then the shorting pin runs the entire width of the patch. In this case, the PIFA is resonant (has maximum radiation efficiency) when:

$$W = L2 \implies L1 = \frac{\lambda}{4} \qquad (1)$$

Suppose that $W = 0$, so that the short is just a pin (or assume $W << L2$). Then the PIFA is resonant at:

$$W = 0 \Longrightarrow L1 + L2 = \frac{\lambda}{4} \qquad (2)$$

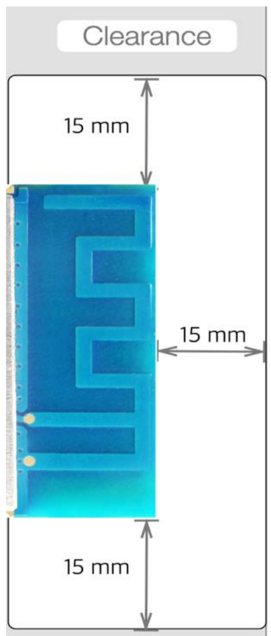

Figure 4.4: Meandered Planar Inverted-F Antenna

In general, the resonant length of a mPIFA as a function of its parameters is approximated as:

$$L1 + L2 - W = \frac{\lambda}{4} \qquad (3)$$

Note that the relationship between frequency, speed of light, and wavelength is represented as:

$$c = \lambda f \qquad (4)$$

Considering the effect of a dielectric with permittivity denoted as ε_r , Eq. (4) will now be represented as:

$$f = \frac{c_0}{\lambda\sqrt{\varepsilon_r}} \quad (5)$$

The PIFA sits on top of a dielectric with permittivity ($\varepsilon_r = 2$) as with the patch antenna.

To obtain the length of the mPIFA, we defined the width $L2$ and shorting pin width as 0.03m and 0.02m respectively.

The frequency we chose for our demonstration is 2400MHz, to avoid interferences with the licensed band. This can be altered for future designs.

Combining Equations (3) and (4) respectively, we obtained a new representation:

$$L1 + L2 - W = \frac{\lambda}{4} = \frac{c}{4f\sqrt{\varepsilon_r}} \quad (6)$$

Applying values in Eq. (6) to obtain the value of $L1$; $L1 + 0.03 - 0.02 = \frac{3\times10^8}{4(2400\times10^6)\sqrt{2}}$

$L1 = 0.017m = 1.7cm.$

From the feed point to the open end along the J-shaped slot, a longer current loop is formed; from the feed point directly to the open end of the mPIFA antenna, a shorter current loop is formed as shown in Fig. 4.4. Tuning the lengths of the two current loops separately can adjust the resonant frequency.

Table 1 shows the important parameters that were considered during the antenna design.

Table 1: Design Parameters

Category	**Value**
Frequency	2400MHz – 2440MHz
Gain	0.97dBi @ 2400MHz
V.S.W. R	< 2.2

Bandwidth	40MHz
Impedance	50 Ohms
Operational Temperature	-45°C ~ 100°C
Radiation Efficiency	62.1% @ 2.44GHz

Frequency: The frequency range chosen as specified in the table is chosen within the 5G S-Band frequency range (2.4GHz). The reason for this is to avoid interference with licensed bands. This can be altered for future designs.

Bandwidth Selection: The Bandwidth decides the frequency response of the antenna. It signifies how well the antenna is matched to the 50-ohm transmission line over the entire band of interest, that is, between 2.40 GHz and 2.44 GHz. The best channel bandwidth range for 5G is 80MHz and 40MHz. 80MHz presents more significant interference, however, 40MHz was used for this work.

Impedance: The key element that influences the Radiofrequency design as against analog design is the impedance of the Radiofrequency circuit. At low frequencies, the impedance of a load remains the same when measured at different distances on the trace from the load. There is also no dependency on the trace width or its uniformity for most applications. Therefore, traces are represented as just nodes at low frequency. But at high frequencies, the impedance (Z) of the Radiofrequency circuit changes when measured at different distances from the load. The change also depends on the substrate used and the dimensions of the Radiofrequency trace. Therefore, the trace also becomes a design element in Radio Frequency schematics.

The key property of a transmission is its characteristic impedance (Z_0), which is the ratio of amplitudes of voltage and current of a wave propagating through a lossless transmission line. For applications at 2.4 – 2.45 GHz such as BLE, a 50-ohm characteristic impedance is widely used for RF traces. Hence a 50-ohm impedance is used in this work.

Gain: The Gain indicates the radiation in the direction of interest compared to the isotropic antenna, which radiates uniformly in all directions. This is expressed in terms of

*d*Bi,(decibel relative to an isotropic radiator) and indicates how strong the radiation field is compared to an ideal isotropic antenna. The value for the designed system is 0.97*d*Bi.

Voltage Standing Wave Ratio (VSWR): The simulated VSWR plot for the antenna is shown in Figure 2. The VSWR or Return Loss determines the matching properties of the antenna. It indicates how efficiently the antenna is transmitting and receiving electromagnetic waves over a particular band of frequencies. The VSWR lies in the range of 1-2.2 for the frequency range 2.4GHz to 2.44GHz, which is within the acceptable range.

Radiation Efficiency: A portion of the non-reflected power gets dissipated as heat or as thermal loss in the antenna. Thermal loss is due to the dielectric loss in the FR4 substrate and the conductor loss in the copper trace. This information is characterized as radiation efficiency. A radiation efficiency of 100 percent indicates that all non-reflected power is radiated to free space. For a small-form-factor PCB, the heat loss is minimal, the radiation efficiency is 62.1%.

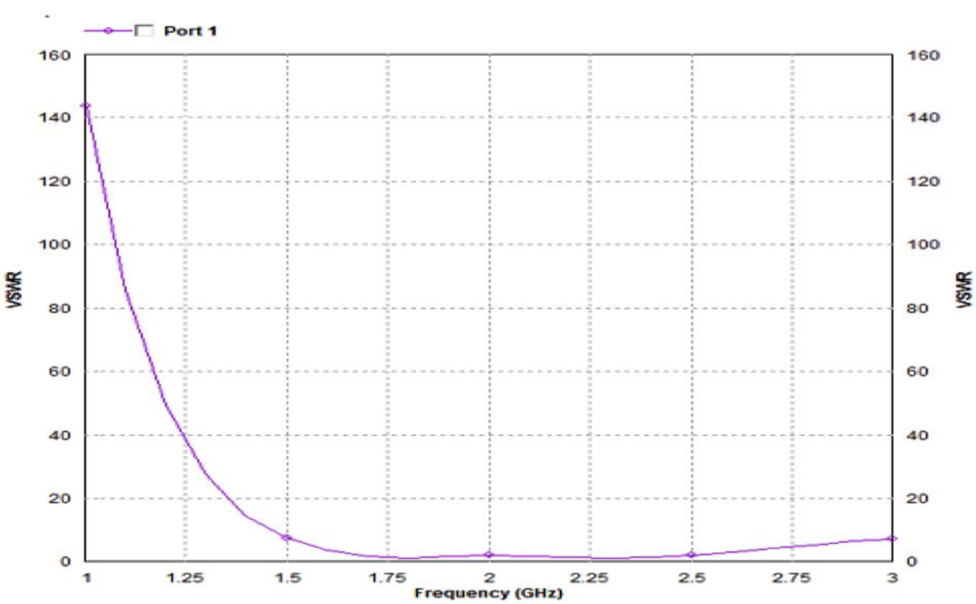

Figure 4.5: Simulated VSWR Plot

Radiation Pattern: The radiation pattern indicates the directional property of radiation, that is, which directions have more radiation and which have less. This information helps to orient the antenna properly in an application. The radiation pattern is tested with a 30-degree angular resolution on a Pioneer Board carrying a module with the mPIFA antenna. The connecting headers are metals and the results are as shown in Fig. 4.6. The radiation is shown more on the z-axis.

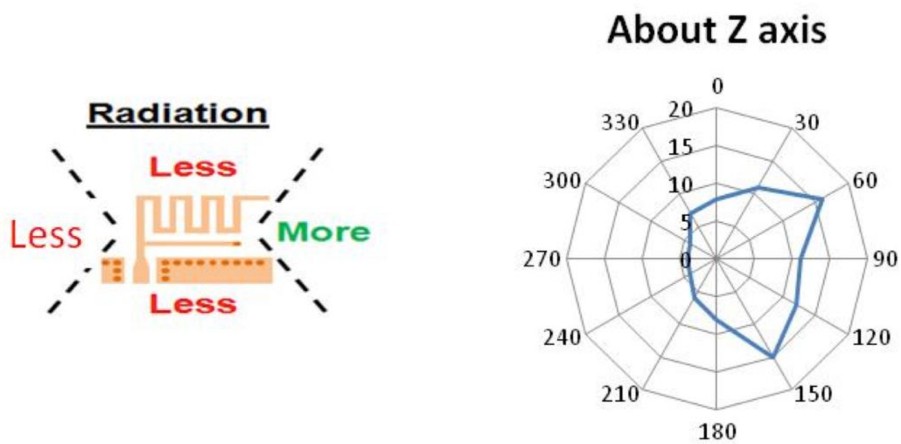

Figure 4.6: Radiation Pattern

4.2.2.2 Multi-Antenna System Design Implementation via Coding

To implement a sequence of the antenna element, the following code snippet is used to configure the radio:

```
Multi.addAP("ssid_from_AP_1", "your_password_for_AP_1");

Multi.addAP("ssid_from_AP_2", "your_password_for_AP_2");

Multi.addAP("ssid_from_AP_3", "your_password_for_AP_3");
```

The above code configures an antenna element and gives it a Service set identifier (SSID) and access key. The snippet further assigns a channel to the created element and carries out isolation to avoid interference. The full code is expected to make all the antenna elements in the multi-antenna system when activated sends pilot signals to the User equipment (UEs) or the receiver unit, which when connected will send feedback to the antenna elements. This feedback represents the channel state information (CSI) of the network. Based on this CSI the multi-antenna system controlled by the coded algorithm loaded in the chips will be able to transmit to the UEs or receiver units through the highest channel quality (i.e. the channel with the best signal-to- noise-and-interference-ratio). Furthermore, to reduce the interference from the fringe area transmitters transmitting in the same channels, a method named frequency offset was used. By this method, a slightly shifted radio frequency is assigned to a transmitter which may experience interference from other transmitters operating in the same channel. The shifted Radio frequency (RF) is calculated by the formula:

$$f_{os} = f_{ch} + \frac{f_L * P}{12} \qquad (7)$$

Where:

f_{os} is the offset RF,

f_{ch} is the standard channel frequency,

P is an integer such that $-12 < p < 0 \; or \; 0 > p > 12$

$f_L f_L$ is the line frequency.

The interference mitigation algorithm as described in our stage 3 deliverable report together with Eq. (7) is written and burnt into the processor of the chipset. This approach will solve the issue of intercell interference/ Resource block collision or co-channel interference.

Figures 4.7 and 4.8 respectively show the manufactured custom PCB designed for the multi-antenna system and the assembled packaged version of the multi-antenna system with embedded transmitters

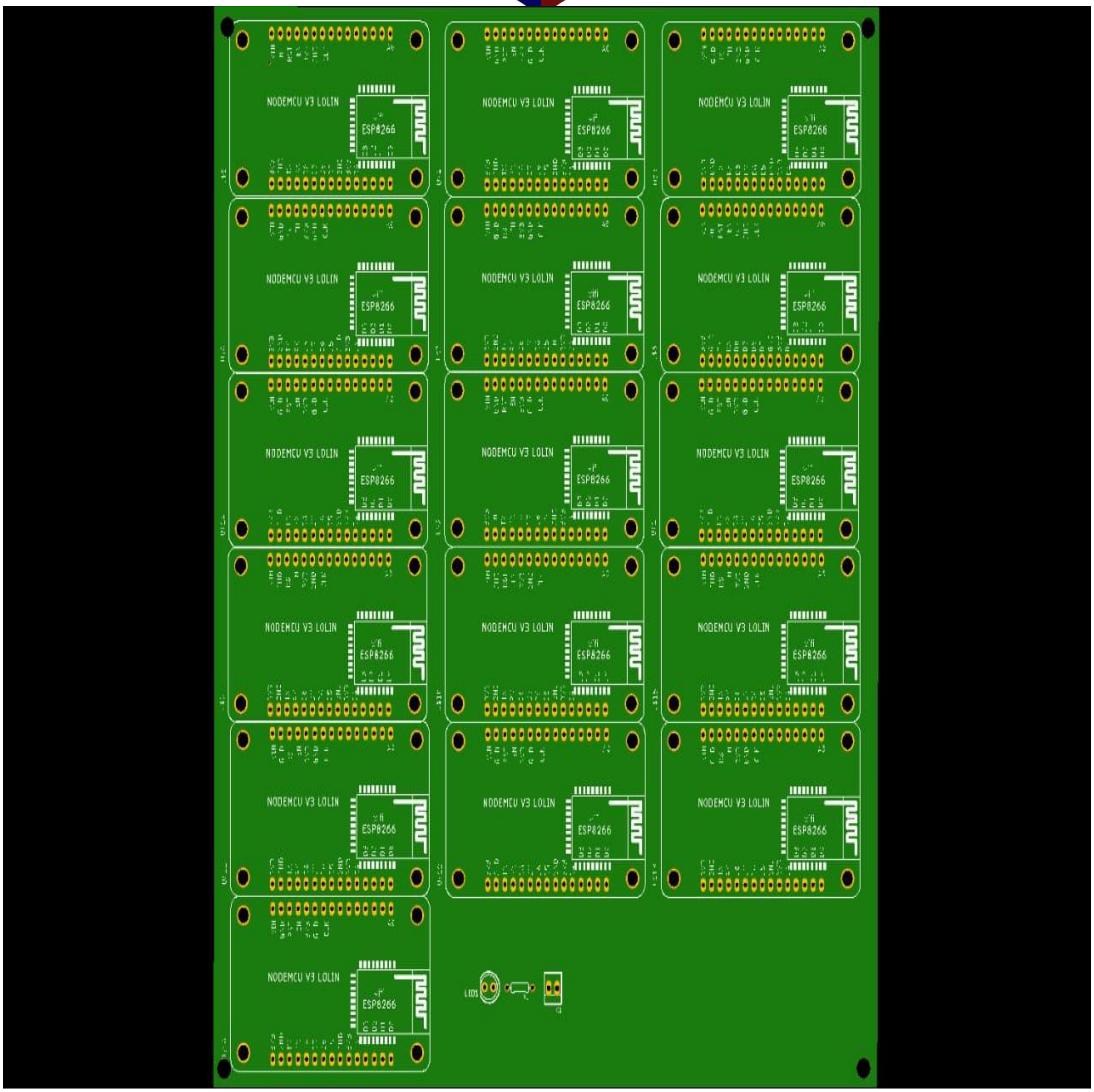

Figure 4.7: Multi-antenna System Custom PCB Design

Figure 4.8: Assembled Package Image of the Multi-Antenna System

4.3 Multi-Antenna System External Power Supply Unit

For 5G, infrastructure OEMs are considering combining the radio, power amplifier (PA), and associated signal processing circuits with the passive antenna array in active antenna units (AAU). While AAUs improve performance and simplify installation, they also require the power supply to share a heatsink with the power amplifier for cooling. In 2G, 3G, and 4G, the power amplifier (PA) and power supply unit (PSU) were separate components, each with its heatsink. In this work, the design considered is based on the integration of a part of the PSU within the radio unit to reduce the radio unit's size and weight and also to have it externally powered. In this architecture, the PSU shares the heatsink with the PA. PAs have

much lower efficiency than PSUs, so their heat will be dissipated into the shared heatsink, raising its temperature and reducing the cooling capability available for the PSU. The reason for powering it externally is also because PSUs that are traditionally operated at temperature ranges exceeding 85ºC result in an increase that could affect component life and performance without compensatory design and manufacturing. Also, note that the PSU integration also increases the risk of signal interference. Being in such proximity to the PA means the PSU must be immune to the E-fields generated by the PA. The PSU generates its E-fields, which must be kept low enough, so they don't affect the PA and other radio frequency electronics.

Let us now look at how the device will dissipate heat in worse-case conditions with a high line voltage of (=230V) and full load. In that scenario, the regulator dissipates the excess power in the form of heat. A regulator has only a maximum amount of power it can dissipate before the internal thermal protection shuts it down or it will be destroyed. Our system is a 5VDC, 2AMP power supply and can be operated at 95V RMS. The power dissipated is calculated as follows:

$$Power = Idc\left(\frac{Vhline}{Vlowline}(Vdc + Vreg) - Vreg\right) \quad (8)$$

$$Power = 2\left(\frac{230}{95}(5 + 3.3) - 3.3\right) = 33.6watts$$

Another important factor considered is the cables used. This work used a pair of low-gauge cables to bring 12V power further regulated to 3.3V to the tower-top radio unit while minimizing voltage drops across them.

Figure 4.9 and Figure 4.10 show the schematic circuit diagram of the external power supply unit and its complete package respectively.

Figure 4.11 shows the two units of the complete package of the multi-antenna system together with the external power source unit mounted on a pole stand. The cables found in the external power source are used to send power to the multi-antenna system units

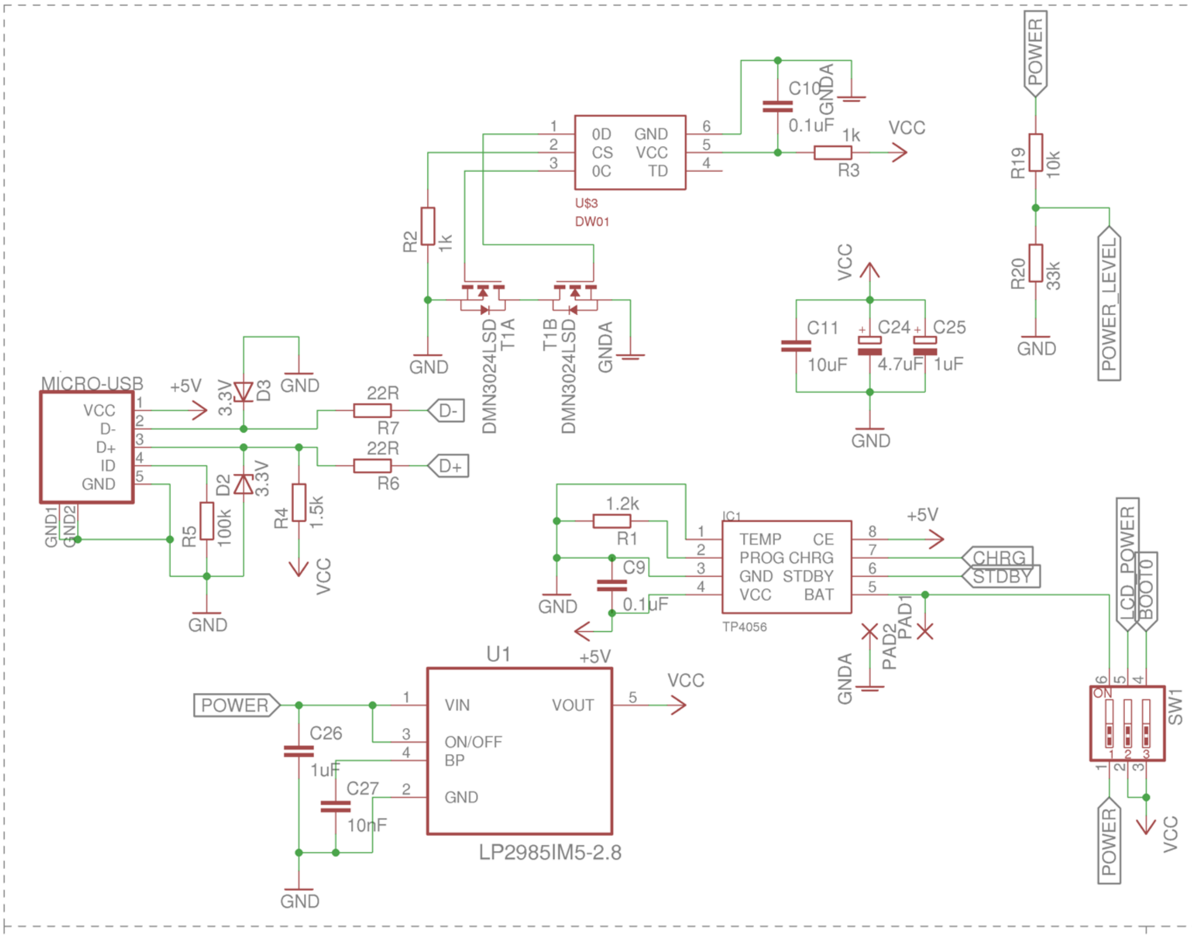

Figure 4.9: Schematic Circuit Diagram of the Power External Unit

Figure 4.10: Image of the complete package of the External Power Supply Unit on a Pole with Cables


5G MASSIVE
MIMO
MADE IN UNIZIK
5G MASSIVE
MIMO
MADE IN UNIZIK

Figure 4.11: Two Units of a Complete Packaged Multi-antenna system connected to an external power source using cable

The multi-antenna system with embedded transmitters cannot on its own demonstrate that the issue of co-channel interference in 5G and other wireless systems has been tackled as a result of the coded algorithm which it implements. Because of this, the prototype will be incomplete without the design and implementation of a receiver (User Equipment) Unit.

4.4 Receiver Unit

To be able to test the operation of the multi-antenna system, a receiver unit was designed to receive and visualize the performance of the multi-antenna system. The receiver module is based on the ESP8266 chipset. The ESP8266 is a low-cost wireless fidelity microchip, with built-in Transmission control protocol/internet protocol (TCP/IP) networking software, and microcontroller capability, produced by Espressif Systems. The module allows microcontrollers to connect to a wireless network and make simple TCP/IP connections using Hayes-style commands. This module was configured to feedback on the CSI of the network back to the multi-antenna system after receiving pilot signals from it. Furthermore, it was configured specifically to receive the signals radiating from the multi-antenna elements and communicate the received signal strength indicator (RSSI) to the display unit. This receiver unit scans for available signals from the antenna element and prints their RSSI (so that you can check that the receiver is connecting to the strongest network on the list). In case it loses connection with the network, it will automatically connect to the next strongest network on the list. The code snippet for this is shown below:

```
if (Multi.run(connectTimeoutMs) == WL_CONNECTED) {
    Serial.print("connected: ");
    Serial.print(SSID());s
    Serial.print(" ");
    Serial.println(.localIP());
  } else {
    Serial.println(" not connected!");
  }
  delay(1000);
```

The schematic circuit diagram of the receiver unit is shown in Fig.4.12

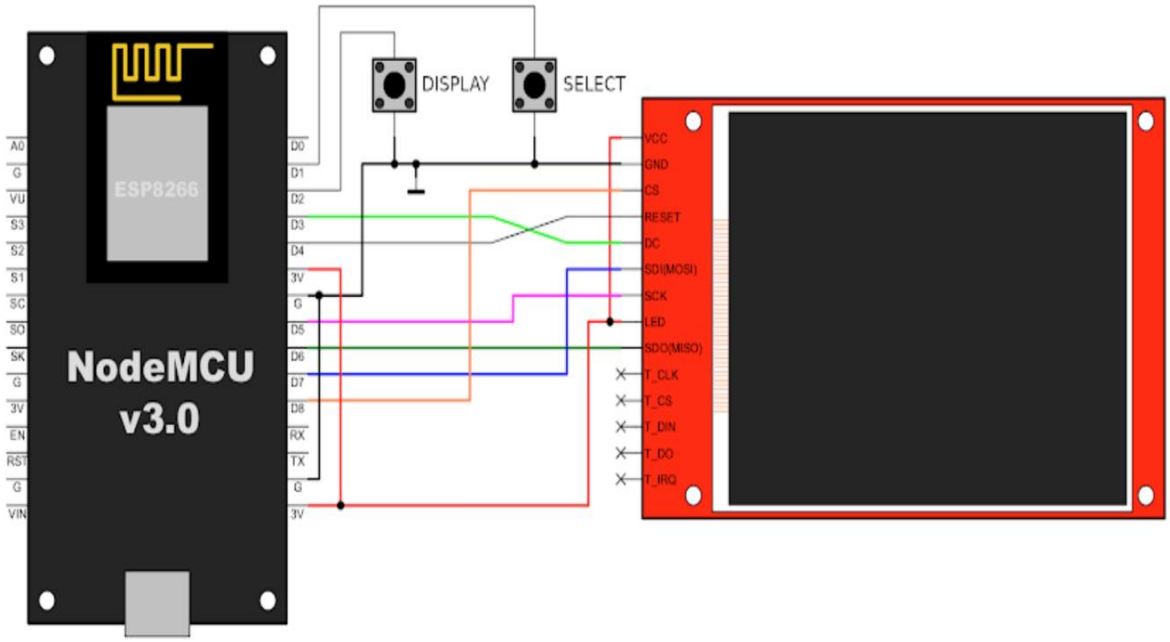

Figure 4.12: Schematic Circuit Diagram for the Receiver Unit

When powered up, a full scan is performed and a list of access points (AP)/ antenna elements is displayed on the screen. Only nine at a time. Unless the AP is hidden, the antenna element SSID is displayed along with the BSSID (MAC address). On the next line, there is a signal indicator and RSSI value in dBm followed by channel and AP security. On the right of the first list item, there is a selection marker that can be moved to the next AP by pressing the SELECT button (assigned to pin D1 of NodeMcu). Keep pressing this button to see all found networks. When you reach the last list element, the next APs will be shown. Each push of the SELECT button delays the next AP scan by 5 seconds. Each new scan resets the list and puts the selection marker on the first item. By the way, access points are sorted by descending RSSI, therefore the nearest will appear on top. Scanning is performed using scanNetworksAsync() function. The image for the scan list is shown in Figure 4.13.

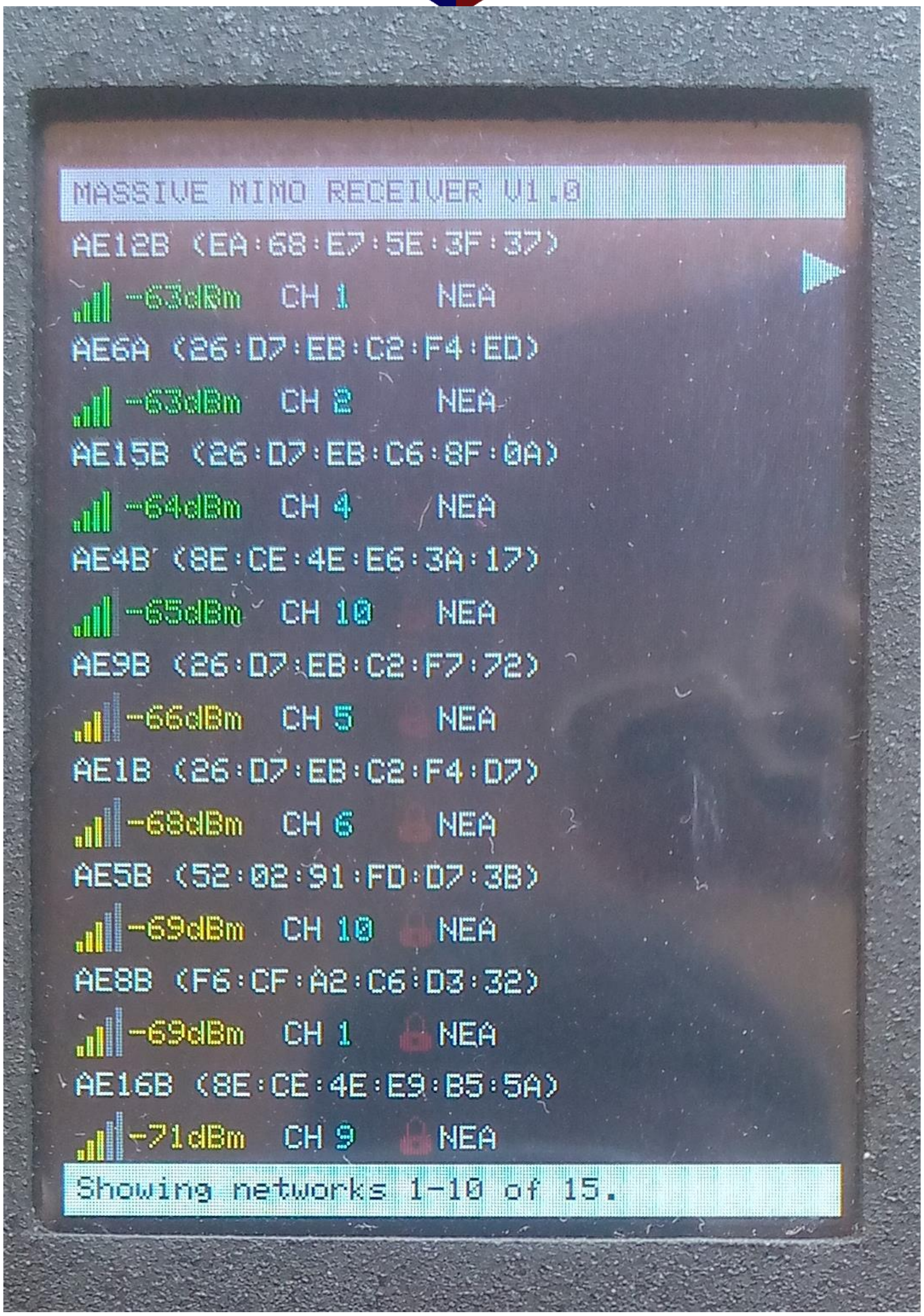

Figure 4.13: Received Unit Scanned List Mode

If you push the DISPLAY button (assigned to pin D2 of NodeMcu), you will see the single network scan screen as shown in Figure 4.14. This mode is useful for monitoring only the selected network (BSSID and channel are used to identify the network you selected in the list).

Besides the big signal indicator, RSSI is also displayed along with an approximation of distance. The presumed distance is calculated in line-of-sight conditions.

In the source code, the structure scan_config holds scan parameters. The scan time is very fast and sometimes misses the AP although it is in range.

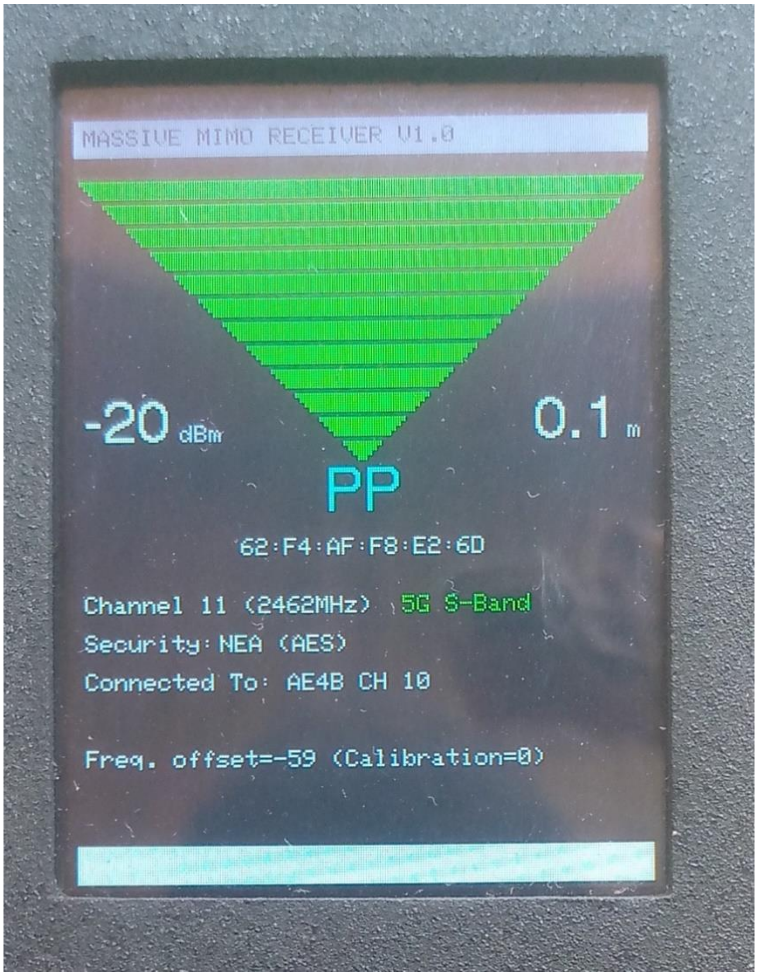

Figure 4.14: Receiver Unit Single Scan Mode

Distance calculation is performed using a formula provided below by code:

```
void approxDistanceToAP(int rssi) {
  int f = selectedChannel * 5 + 2407;
  if (selectedChannel == 14) f = 2484;
  rssi = abs(rssi);
  double ex = (27.55 - (20 * log10(f)) + rssi) / 20;
  float dist = pow(10, ex);
  String sdist = String(dist, 1);
  if (rssi == 100) sdist = "--";

  tft.setTextDatum(R_BASELINE);
  tft.setTextPadding(64);
  tft.setTextColor(TFT_WHITE, TFT_BLACK);
  tft.drawString(sdist, 226, 136, 4);
  tft.setTextDatum(R_BASELINE);
  tft.setTextPadding(0);
  tft.setTextColor(TFT_LIGHTGREY, TFT_BLACK);
  tft.drawString("m", 236, 129, TEXT_FONT);
}
```

The PCB design of the receiver unit is shown in Figure 4.15 while the complete package view of the receiver unit is shown in Figure 4.16:

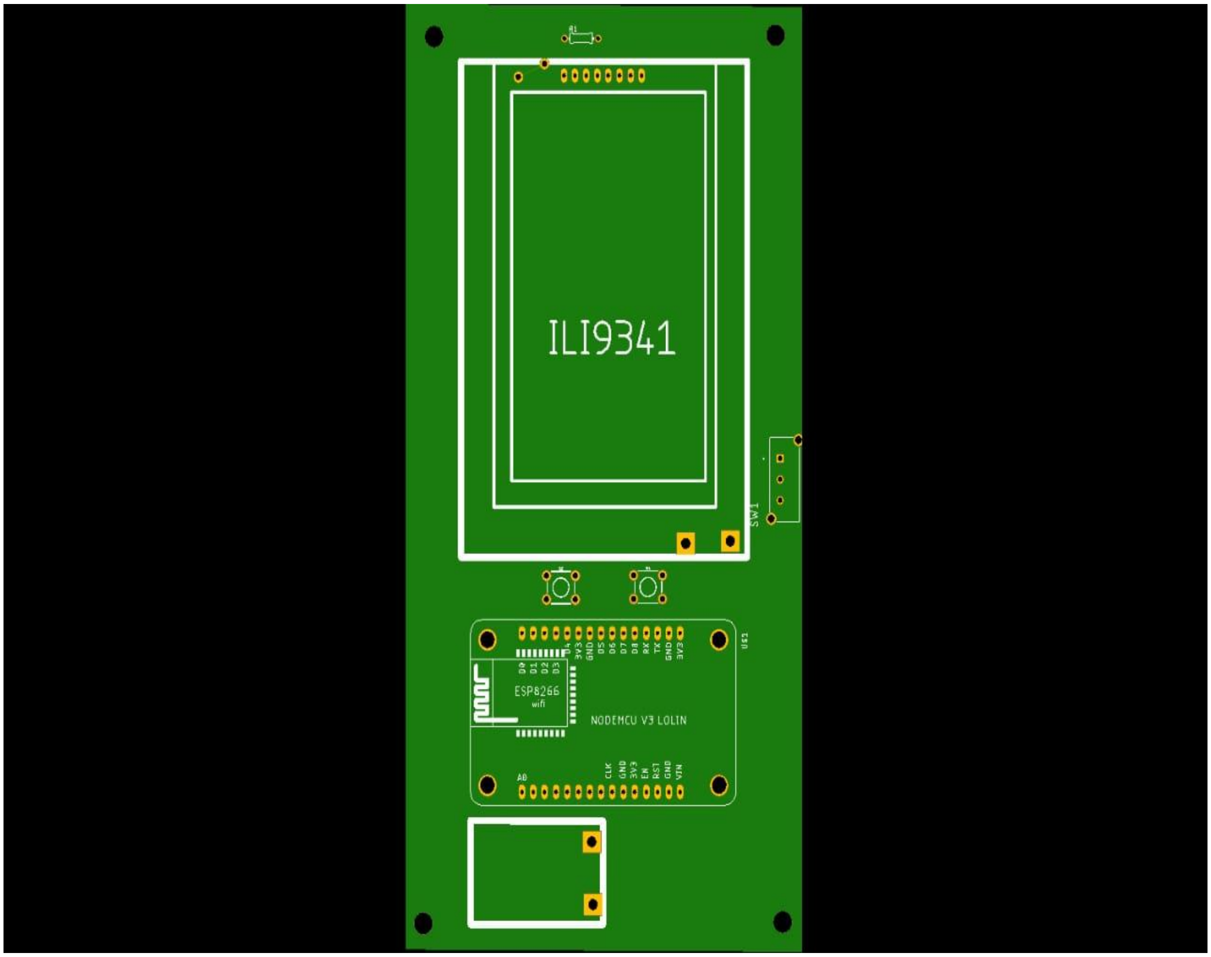

Figure 4.15: The PCB Design of the Receiver Unit

To view the interaction between the transmitters and the receivers in this work in the form of signals transmitted and received, the network visualizer unit was devised and developed. Figure 4.17 and Figure 18 show the schematic circuit diagram of the network visualizer unit and the complete package of the devised network visualizer unit respectively. This is important because, without this unit, characterization of the network will be difficult.

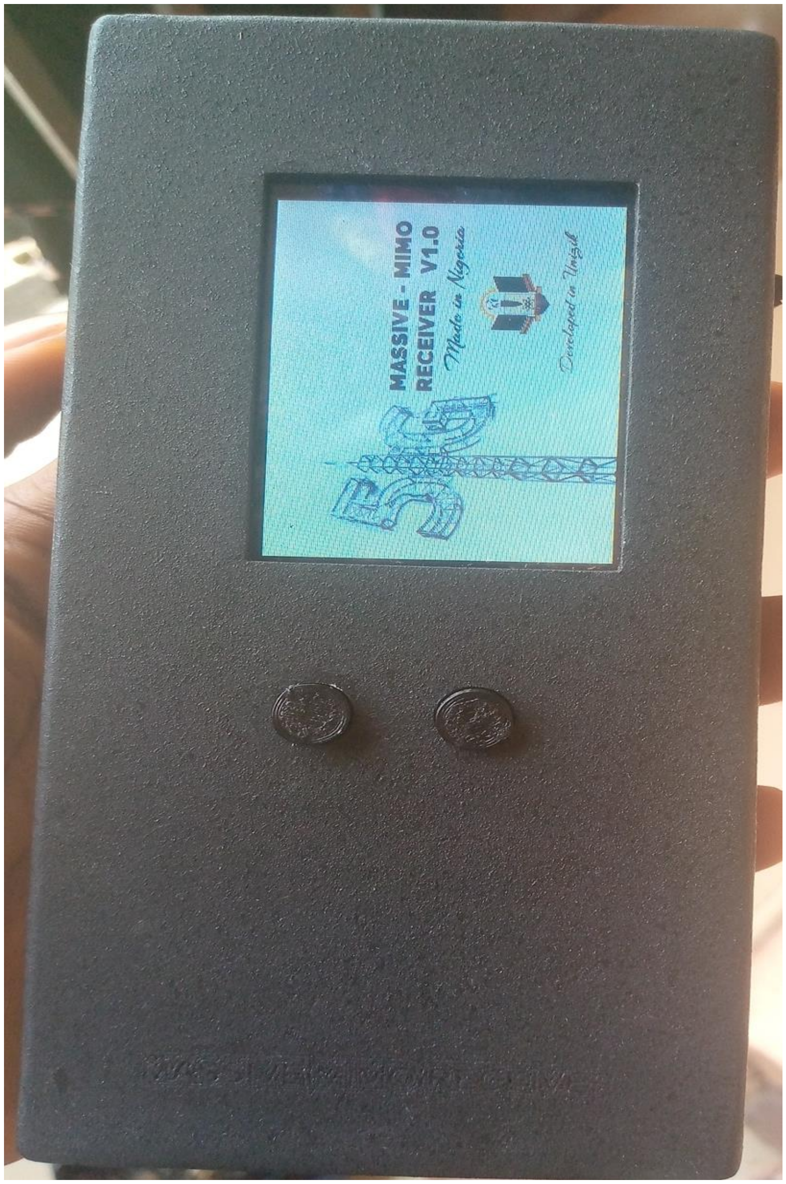

Figure 4.16: Package View of the Receiver Unit

4.5 Network Visualizer Unit

The Visualizer is a handheld Radio frequency spectrum analyzer that includes both hardware and software. It interfaces with a personal computer running the Arduino IDE software and can also work standalone when powered by a reliable 5V power source.

The wideband, Radiofrequency spectrum analyzer spans a frequency range of 2400MHz up to 2660 MHz, which makes it ideal for use in a broad array of Radio frequency-related applications. The visualizer employs a USB dongle based on the Xtens 32-bit LX6, chipset that supports a USB 2.0 interface. In this work, it is configured as a Software Defined Radio (SDR). The code snippet for carrying out the visualization is shown below:

```
int n = WiFi.scanNetworks();
  // clear old graph
  tft.fillRect(0, BANNER_HEIGHT, 320, 224, TFT_BLACK);
  tft.setTextSize(1);
  if (n == 0) {
    tft.setTextColor(TFT_BLACK);
    tft.setCursor(0, BANNER_HEIGHT);
    tft.println("no networks found");
  } else {
    // plot found WiFi info
    for (int i = 0; i < n; i++) {
      int32_t channel = net.channel(i);
      int32_t rssi = net.RSSI(i);
      uint16_t color = channel_color[channel - 1];
      int height = constrain(map(rssi, RSSI_FLOOR, RSSI_CEILING, 1, GRAPH_HEIGHT), 1, GRAPH_HEIGHT);
      // channel stat
      ap_count[channel - 1]++;
      if (rssi > max_rssi[channel - 1]) {
```

```
        max_rssi[channel - 1] = rssi;
      }
// print WiFi stat
  tft.setTextColor(TFT_WHITE);
  tft.setCursor(0, BANNER_HEIGHT);
  tft.print(n);
  tft.print(" networks found, suggested channels: ");
  bool listed_first_channel = false;
  for (int i = 1; i <= 11; i++) { // channels 12-14 may not available
    if ((i == 1) || (max_rssi[i - 2] < NEAR_CHANNEL_RSSI_ALLOW)) { // check previous channel signal strength
      if ((i == size of(channel_color)) || (max_rssi[i] < NEAR_CHANNEL_RSSI_ALLOW)) { // check next channel signal strength
        if (ap_count[i - 1] == 0) { // check no AP exists in same channel
          if (!listed_first_channel) {
            listed_first_channel = true;
          } else {
            tft.print(", ");
          }
          tft.print(i);
        }
      }
    }
  }
```

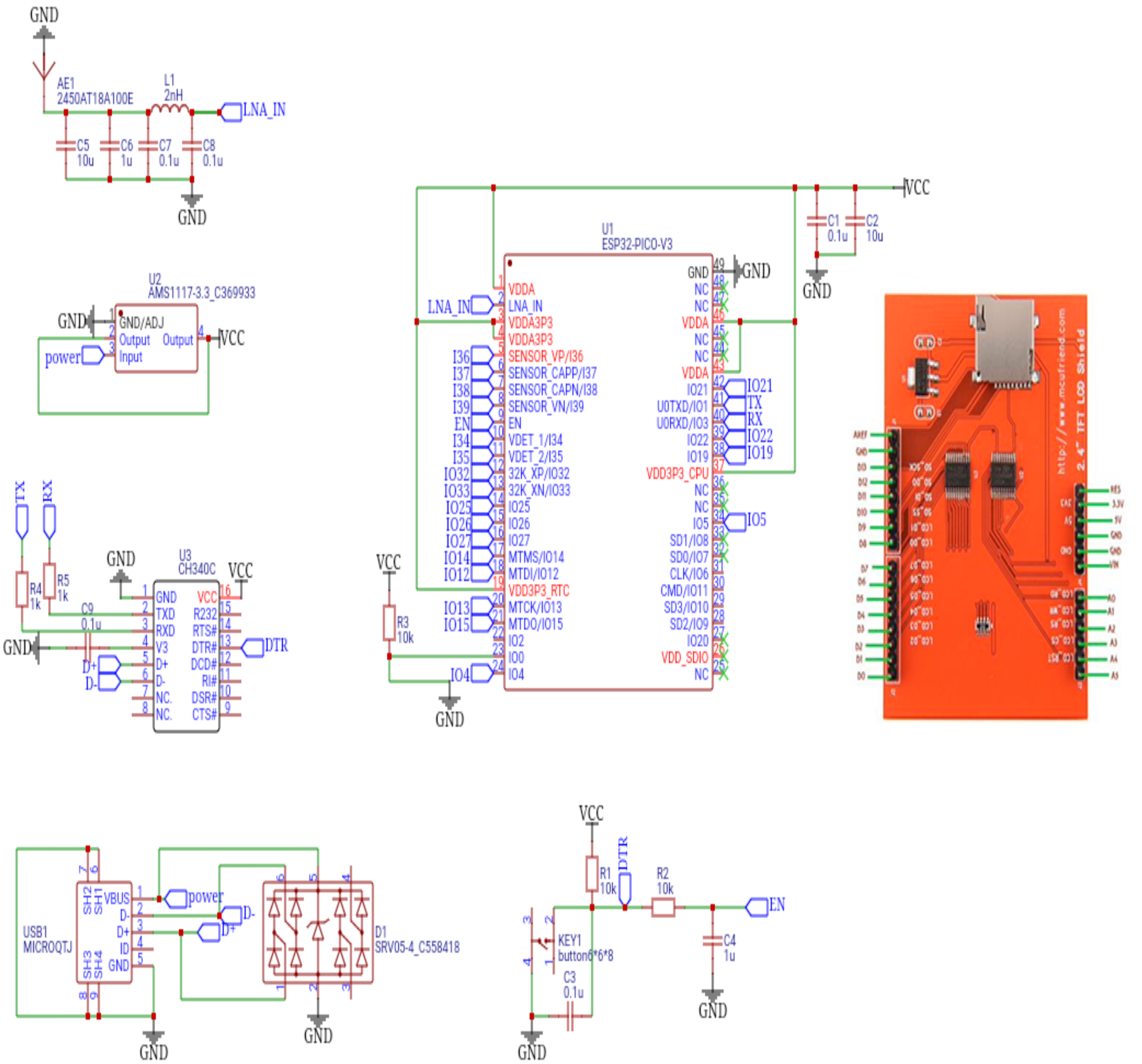

Figure 4.17**:** Schematic Circuit Diagram for the Network Visualizer

Figure 4.18: Complete Package of the Network Visualizer Unit

SECTION FIVE: SUMMARY AND CONCLUSION

5.1 Summary of Findings

We found out that our proposed method if applied to the design of the fifth-generation mobile communication system would be able to achieve the following:

I. The theoretical minimum achievable spectral efficiency which is 30 bits/s/Hz at the following baseline parameters: Base station having 4 antenna elements, serving 4 users at SNR of 30dB.

II. Extra 13bits/s/Hz when the number of antenna elements at the base stations increases to 12 from 4 at the same number of users = 4, and SNR = 30dB.

III. Extra 18 bits/s/Hz when the number of antenna elements at the base stations increases to 20 from 4 at the same number of users = 4, and SNR = 30dB.

IV. Extra 65 bits/s/Hz when the number of antenna elements at the BSs increases to 20 from 4 at an increased number of users = 9, and SNR = 30 dB.

V. Compare (III) and (IV) there will be an extra gain of 47 bits/s/Hz when the number of users increases to 9 from 4 at the same SNR = 30dB and antenna elements at base stations = 20.

5.2 Conclusion

The spectral efficiency of a 5G network can be improved by increasing the number of antenna elements in the base stations and increasing the number of users the antenna elements are utilized to serve simultaneously. That is after the significant interfering signals emanating from neighboring base stations are dealt with using our devised methods: A user-centric clustering scheme and an optimal resource allocation scheme.

Acronyms

The following acronyms and abbreviations were used in this report:

BS	Base Station
B5G	Beyond 5G
CB	Coordinated Beamforming
CRAN	Cloud Radio Access Network
CRE	Cell Range Expansion
CSI	Channel State Information
EICIC	Enhanced Inter-cell Interference Coordination
ICI	Inter-cell Interference
ICIC	Inter-cell Interference Coordination
JT	Joint Transmission
MBS	Macro Base Station
MCP	Multi-Cell Processing
MIMO	Multiple-Input Multiple-Output
OFDM	Orthogonal Frequency Division Multiplexing
OPEX	Operational Expenditures
PBS	Pico Base Station
RA	Resource Allocation
RSRP	Reference Signal Receive Power
SCBS	Small Cell Base Stations
SCP	Single Cell Processing
SDMA	Space-Division Multiple Access
SE	Spectral Efficiency
SINR	Signal-to-Interference-and-Noise-Ratio
UE	User Equipment
3GPP	Third Generation Partnership Project
5G	Fifth-Generation Mobile Communication Network
K_{m}	Total number of UEs in the system for downlink transmission

N Total number of transmit (receive) antenna in each cell for downlink (uplink) transmission

M Total number of UEs in the cell for uplink transmission.

REFERENCES

[1] Gupta, A. and Jha, R.K., "A survey of 5G Network: Architecture and emerging technologies." *IEEE Access*, 2015, **3**, 1206 – 1232.

[2] Nam, W., Bai, D., Lee, J., *et al.*: 'Advanced interference management for 5G cellular networks', *IEEE Commun. Mag.*, 2014, **52**, (5), pp. 52–60

[3] Chin, W., Fan, Z., Haines, R.: 'Emerging technologies and research challenges for 5G wireless networks', *IEEE Wirel. Commun.*, 2014, **21**, (2), pp. 106–112

[4] Oguejiofor, O., Zhang, L.: 'Heuristic coordinated beamforming for heterogeneous cellular network'. Proc. IEEE 83rd Vehicular Technology Conf. (VTC Spring), Nanjing, China, May 2016, pp. 1–5

[5] Irmer, R., Droste, H., March, P., *et al.*: 'Coordinated multipoint: concepts, performance, and field trial results', *IEEE Commun. Mag.*, 2011, **49**, (2), pp. 102–111

[6] R1-111282: 'Performance evaluation of CoMP JT for scenario 2'. Available at http://www.3gpp.org/DynaReport/TDocExMtg–R1-65–28504.htm, accessed January 2021.

[7] R1-111290: 'CoMP phase 1 evaluation results'. Available at http://www.3gpp.org/DynaReport/TDocExMtg–R1-65–28504.htm, accessed January 2021.

[8] R1-111277: 'CoMP JT evaluation for phase 1 homogenous deployment'. Available at http://www.3gpp.org/DynaReport/TDocExMtg–R1-65–28504.htm, accessed January 2021.

[9] Zhu, L. et al., "Cluster-based energy-efficient joint user association and resource allocation for B5G ultra-dense networks." *Physical Communication.*2021, **46**: 101311.

[10] Prabakar, D. and Saminadam, V., "MMC-DIA: Multi-metric Clustering with differential interference alignment for improving small cell performance." *Journal of Ambient Intelligence and Humanized Computing*, 2021, **12** (2), pp. 2495 -2507.

[11] R1-090140: 'Clustering for CoMP transmission'. Available at http://www.3gpp.org/DynaReport/TDocExMtg–R1-55b–27322.htm, accessed January 2021.

[12] Dahrouj, H., Yu, W.: 'Coordinated beamforming for the multicell multiantenna wireless system', *IEEE Trans. Wirel. Commun.*, 2010, **9**, (5), pp.1748–1759

[13] Karakayali, M., Foschini, G., Valenzuela, R.: 'Network coordination for spectrally efficient communications in cellular systems', *IEEE Wirel.Commun. Mag.*, 2006, **13**, (4), pp. 56–61

[14] Gesbert, D., Kiani, S., Gjendemsjo, A., *et al.*: ‘Adaptation, coordination, and distributed resource allocation in interference-limited wireless networks’,*Proc. Inst. Elect. Electron. Eng.*, 2007, **95**, (12), pp. 2393–2409

[15] Han, T., Kobayashi, K.: ‘A new achievable rate region for the interference channel’, *IEEE Trans. Inf. Theory*, 1981, **27**, (1), pp. 49–60

[16] Liu, Y.F., Dai, Y.H.: ‘Coordinated beamforming for MISO interference channel: complexity analysis and efficient algorithms’, *IEEE Trans. Signal Process.*, 2011, **59**, (3), pp. 1142–1157

[17] Shang, X., Chen, B., Poor, H.V.: ‘Multiuser MISO interference channels with single-user detection: optimality of beamforming and the achievable rate region’, *IEEE Trans. Inf. Theory*, 2011, **57**, (7), pp. 4255–4273

[18] Mayer, H., Schlesinger, H.: ‘Antenna synchronization for coherent network MIMO’, U.S. Patent 20120002967, March 2010

[19] Dai, B., Yu, W.: ‘Sparse beamforming and user-centric clustering for downlink cloud radio access network’, *IEEE Access.*, 2014, **2**, pp. 1326–1339

[20] Nigam, G., Minero, P., Haenggi, M.: ‘Coordinated multipoint joint transmission in heterogeneous networks’, *IEEE Trans. Commun.*, 2014, **62**, (11), pp. 4134–4146

[21] Tanbourgi, R., Singh, S., Andrews, J., *et al.*: ‘Analysis of non-coherent joint transmission cooperation in heterogeneous cellular networks’. Proc. IEEE Int. Conf. on Communications (ICC), Sydney, NSW, Australia, June 2014, **3**, 5160–5165

[22] Wyner, A.: ‘Shannon-theoretic approach to a Gaussian cellular multiple access channel’, *IEEE Trans. Inf. Theory*, 1994, **40**, (6), pp. 1713–1727

[23] Gesbert, D., Hanly, S., Huang, H., *et al.*: ‘Multi-cell MIMO cooperative networks: a new look at interference’, *IEEE J. Sel. Areas Commun.*, 2010, **28**, (9), pp. 1380–1408

[24] Shamai, S., Zaidel, B.: ‘Enhancing the cellular downlink capacity via co-processing at the transmitting end’. Proc. IEEE Vehicular Technology Conf. (VTC), Rhodes, Greece, May 2001, **3**, pp. 1745–1749

[25] Huang, H., Trivellato, M., Hottinen, A., *et al.*: ‘Increasing downlink cellular throughput with limited network MIMO coordination’, *IEEE Trans. Wirel.Commun.*, 2009, **8**, (6), pp. 2983–2989

[26] Marsh, P., Fettweis, G.: ‘On multicell cooperation transmission in backhaul constrained cellular system’, *Ann. Telecommun.*, 2008, **63**, pp. 253–269

[27] Marsh, P., Fettweis, G.: ‘Static clustering for cooperative multi-point (CoMP) in mobile communication’. Proc. IEEE Int. Conf. on Communications (ICC), Kyoto, Japan, July 2011, pp. 1–6

[28] Wang, H., Zhou, X., Reed, M.: ‘Coverage and throughput analysis with non-uniform small cell deployment’, *IEEE Trans. Wirel. Commun.*, 2014, **13**, (4), pp. 2047–2059

[29] Akoum, S., Health, R.W.: ‘Interference coordination: random clustering and adaptive limited feedback’, *IEEE Trans. Signal Process.*, 2013, **61**, (7), pp. 1822–1834

[30] Li, C., Zhang, J., Haenggi, M., *et al.*: ‘User-centric inter-cell nulling for downlink small cell networks’, *IEEE Trans. Commun.*, 2015, **63**, (4), pp.1419–1431

[31] Afshang, M., Dhillon, H., "A New Clustered HetNet Model to Accurately Characterize User-Centric Small Cell Deployments," *IEEE Wireless Communications and Networking Conference (WCNC)*, 2017, pp. 1-6.

[32] Chen, Y., Lu, Z., Wen, X., *et al.*: ‘User-centric clustering and beamforming for energy optimization in cloud RAN’, *Mob. Netw. Appl.*, 2018, **23**, (3), pp.503–517

[33] Hu, B., Hua, C., Chen, C. and Guan, X.: “Joint beamformer design for wireless fronthaul and access links in C-RANs,” *IEEE Transactions on Wireless Communications*, 2018, **17**, (5), pp.2869-2881.

[34] Khalili, A., Akhlaghi, S., Hoseni, S.A.: ‘Joint resource allocation and antenna selection in the uplink of OFDMA networks’, arXiv:1801.02688, 2018

[35] Khalili, A., Akhlaghi, S., Mirzaee, M.: ‘Asymptotic close to optimal joint resource allocation and power control in the uplink of two-cell networks’, arXiv:1711.07913, 2017

[36] Zhang, X., Su, Z., Yan, Z., *et al.*: ‘Energy-efficiency study for two-tier heterogeneous networks (HetNet) under coverage performance constraints’, *Mob. Netw. Appl.*, 2013, **18**, (4), pp. 567–577

[37] Huang, Y., Zhang, X., Zhang, J., *et al.*: ‘Energy-efficient design in heterogeneous cellular networks based on large-scale user behavior constraints’, *IEEE Trans. Wirel. Commun.*, 2014, **13**, (9), pp. 4746–4757

[38] Soh, Y., Quek, T., Kountouris, M., *et al.*: "Energy efficient heterogeneous cellular networks", *IEEE J. Sel. Areas Commun.*, 2013, **31**, (5), pp. 840–850

[39] Khan, H.Z., Ali, M., Rashid, I., Ghafoor, A., Naeem, M., Khan, A.A. and Saddiqui, A.M.: "Resource allocation for energy efficiency optimization in uplink–downlink decoupled 5G heterogeneous networks", *International Journal of Communication Systems*, 2021, *34,* (14), p.e4925.

[40] Shahzad, F., Ali, M., Zubair Khan, H., Naeem, M., Masud, U. and Qamar, F.: " Joint user association and energy efficiency maximization in beyond 5G heterogeneous networks," *International Journal of Communication Systems*, 2022, **35**, (8), p.e5122.

[41] Xu, Y., Gui, G., Gacanin, H. and Adachi, F.: "A survey on resource allocation for 5G heterogeneous networks: Current research, future trends, and challenges," *IEEE Communications Surveys & Tutorials*, 2021, **23**, (2), pp.668-695.

[42] Uguru, S., Idigo, V., Oguejiofor, O.S.: "Enhanced Interference Management Technique for Multi-cell Multi-Antenna System", *International Journal of Electronics and Communication Engineering*. 2021, **15**, (11), pp. 376-381.

[43] Oguejiofor, O., Zhang, L., Nawaz, N.: "Heterogeneous Networks: Optimization, Resource Allocation, and Interference Management Techniques," Ibadan, Nigeria. University Press Plc, pp. 1-160, 2021.

[44] Oguejiofor, O., Abe, A., Aniedu, A.: "Interference Issues and Management Techniques in Heterogeneous Cellular Networks: A Review," *IUP Journal of Telecommun*., 2018, **10**, (4), pp. 7 – 28.

[45] Oguejiofor, O.S.: "Enhanced Interference Management Techniques for Heterogeneous Cellular Networks," Ph.D. Thesis, School of Elect. And Electron. Engrn. Univ. Leeds, Leeds, 2017.

[46] Mohanad, A., Zhang, L., Oguejiofor, O.: "Inbound Handover Interference-Based Margin for load Balancing in Heterogeneous Networks," in *proc. 14th International Symposium on Wireless Communication Systems (ISWCS)*. Bologna, Italy, Aug. 2017, pp. 1--6.

[47] Oguejiofor, O., Zhang, L., Nawaz, N.: “Resource Allocation for Practical Two-Tier Heterogeneous Cellular Networks," in *proc. 23rd European Wireless (EW).* Dresden, Germany, May 2017, pp. 1--6.

[48] Oguejiofor, O., Zhang, L., Mohanad, A.: “Decentralized Resource Allocation for Heterogeneous Cellular Networks,” in *proc. 14th International Symposium on Wireless Communication Systems (ISWCS)*. Bologna, Italy, Aug. 2017, pp. 1--6.

[49] Oguejiofor, O., Abe, A., Aniedu, A.: “Distributed Resource Allocation for two-tier Heterogeneous Cellular Networks,” *IUP Journal of Telecommun*., 2018, **10**, (2), pp. 7—33.

[50] Idigo, V., Azubogu, A., Ohaneme, C., Oguejiofor, O.: “Evaluation of Beamforming Algorithm for smart antenna system**,**” *IUP Journal of Telecommunications (IJT),* 2013, **5**, (1), pp. 29--45.

[51] K. Okino, T. Nakayama, C. Yamazaki, H. Sato, and Y. Kusano, “Pico cell range expansion with interference mitigation toward LTE-Advanced heterogeneous networks,” in *proc. IEEE Int. Conf. Commun. Workshops (ICC)*, 2011, pp. 1–5.

[52] G. Scutari, D. P. Palomar, and S. Barbarossa, “Cognitive MIMO radio,” *IEEE Signal Process. Mag.*, vol. 25, no. 6, pp. 46–59, 2018.

[53] Y. Huang and D. P. Palomar, “Rank-constrained separable semidefinite programming with applications to optimal beamforming,” *IEEE Trans. Signal Process.*, vol. 58, no. 2, pp. 664–678, 2010.

[54] S. K. Joshi, P. C. Weeraddana, M. Codreanu, and M. Latva-Aho, “Weighted sum-rate maximization for miso downlink cellular networks via branch and bound,” *IEEE Trans. Signal Process.*, vol. 60, no. 4, pp. 2090–2095, 2012.

[55] A. Wiesel, Y. C. Eldar, and S. Shamai, “Linear precoding via conic optimization for fixed MIMO receivers,” *IEEE Trans. Signal Process.*, vol. 54, no. 1, pp. 161–176, 2006.

[56] M. Bengtsson and B. Ottersten, “Optimal and suboptimal transmit beamforming.”CRC Press, 2011.

[57] J. F. Sturm, “Using SeDuMi 1.02, a MATLAB toolbox for optimization over symmetric cones,” *Optimization methods and software*, vol. 11, no. 1-4, pp. 625–653, 1999.

[58] M. Grant and S. Boyd, “CVX: Matlab software for disciplined convex programming, version 2.2,” 2020